Fabrication of AlGaN/GaN MESFET And It's Applications in Biosensing

by

Siddharth Alur

A dissertation submitted to the Graduate Faculty of
Auburn University
in partial fulfillment of the
requirements for the Degree of
Doctor of Philosophy

Auburn, Alabama
December 13, 2010

Keywords: AlGaN/GaN, HEMT, MESFET, PDMS, DNA, Hybridization, OPH

Approved by

Minseo Park, Chair, Associate Professor of Physics
John R. Williams, Professor of Physics
Michael J. Bozack, Professor of Physics
Dong-Joo Kim, Associate Professor of Materials Engineering
Tung-Shi Huang, Assitant Professor of Nutrition and Food Sciences

Abstract

Gallium Nitride has been researched extensively for the past three decades for its application in Light Emitting Diodes (LED's), power devices and UV photodetectors. With the recent developments in crystal growth technology and the ability to control the doping there has been an increased interest in heterostructures formed between Gallium nitride and it's alloy Aluminium Gallium Nitride. These heterostructures due to the combined effect of spontaneous and piezoelectric effect can form a high density and a high mobility electron gas channel without any intentional doping. This high density electron gas makes these heterostructures ideal to be used as sensors. Gallium Nitride is also chemically very stable.

Detection of biomolecules in a fast and reliable manner is very important in the areas of food safety and medical research. For biomolecular detection it is paramount to have a robust binding of the probes on the sensor surface.

Therefore, in this dissertation, the fabrication and application of the AlGaN/GaN heterostructures as biological sensors for the detection of DNA and Organophosphate hydrolase enzyme is discussed. In order to use these AlGaN/GaN heterostructures as biological sensors capable of working in a liquid environment photodefinable polydimethyl-siloxane is used as an encapsulant. The immobilization conditions for a robust binding of thiolated DNA and the catalytic receptor enzyme organophosphate hydrolase on gold surfaces is developed with the help of X-ray photoelectron spectroscopy. DNA and OPH are detected by measuring the change in the drain current of the device as a function of time.

Acknowledgments

The author would like to give deepest appreciation to Dr. Minseo Park for his guidance, advice and support through the entire research work during the Ph.D period at Auburn University. The author also would like to give thanks to all the committee members, Dr. John Williams, Dr. Michael J. Bozack, Dr. Kim, Dr. Tsung Shi Hung and Dr. Ahjeong Son for their participation in evaluating the work.

Additional, the author would like to thank Dr. Claude Ahyi for his kindly help and discussion every time. Thanks to Tamara Isaacs-Smith for her assistance with the experimental setups and with correcting this dissertation. Thanks to Yaqi Wang, Tony Gnanaprakasa, Saroja Mantha and Xingguang Zhu for discussion of problems with the biomolecular immobilization and device fabrication procedures.

Finally, the author would like to express special thanks to his sister Pallavi Alur for her guidance and encouragement. The author would also like to thank his parents for their support.

Table of Contents

List of Tables

List of Figures

List of Abbreviations

DNA	Deoxy Ribo Nucleic Acid
OPH	Organo Phosphate Hydrolase
HEMT	High Electron Mobility Transistor
MUA	MercaptoUndecanoic Acid
OP	Organo Phosphate
XPS	X-Ray Photoelectron Spectroscopy
MESFET	Metal Semiconductor Field Effect Transistor

CHAPTER 1

Introduction

1.1 Nitride semiconductors

Over the last three decades group III nitrides semiconductor materials have been studied extensively for their applications in Light Emitting Diodes (LED's), high temperature/power devices and chemical, gas and biological sensors[1-3]. Some of the common group III nitrides semiconductors are Gallium nitride (GaN), Indium nitride (InN), Boron nitride (BN) and Aluminum gallium nitride (AlGaN). The first Gallium Nitride (GaN) based light emitting diode was reported in the 1970's[4]. The pioneering research on nitride semiconductors by Pankove, Akasaki, Nakamura and many others established the potential applications of these semiconductors in optoelectronics. Later in 1991 the first nitride based field effect transistor was fabricated[5]. A large band gap discontinuity of 3.39eV, a high peak electron velocity, saturation velocity (3 $X10^7$ cm/sec) and a high thermal and chemical stability are the primary reasons that enable the use of nitride semiconductors to be used in high temperature, voltage and high power devices. Another unique property is the excellent chemical stability of GaN. GaN has no known wet etchants. This is the reason why FET's of GaN and its alloy AlGaN is also used as biosensors.

The group III-N semiconductors can exist in three crystal structures Wurzite, Zinc blende and rock salt structure. In ambient conditions the thermodynamically stable structure for bulk GaN, AlN and InN is the wurtzite crystal structure. GaN, AlN and InN can be grown in the rock salt structure under very high pressure. In the wurzite structure GaN, AlN and InN have a band gap of 3.4, 6.2 and 1.9 eV respectively at room temperature[6]. As shown in the figure (figure 1) a wurtzite crystal structure consists of 2 interpenetrating hexagonal close packed structures each with one type of atom offset along the c axis by 5/8 of the cell height[7].

It was only in the 1990's that a high quality defect free GaN was successfully grown using Metal Organic Chemical Vapor Deposition (MOCVD). These procedures used either GaN or AlN as nucleation materials[8-9]. As the growth methods improved and the unintentional doping was reduced, it was possible to do intentional doping. Silicon and Germanium were used for n-type doping of GaN. Initially there were a few setbacks in the p-type doping of GaN. These problems were overcome by Amano et al[10] who used Magnesium to dope GaN p type by Low Energy Electron Beam Irradiation (LEEBI). GaN and AlN are chemically and thermally very stable. Even though their thermal stability is exploited in high temperature devices their chemical stability posses certain difficulties since the well established wet processes cannot be applied to them.

We have to use only dry etching during their processing. Cl_2 based discharge is commonly used to etch GaN. GaN and its alloy AlGaN form heterostructures that offer a high mobility (>1300cm^2/v-sec) and a high density electron gas (1X $10^{13}/cm^2$) without any intentional doping. This property is useful in application ranging from chemical and biological sensors to fast switching devices.

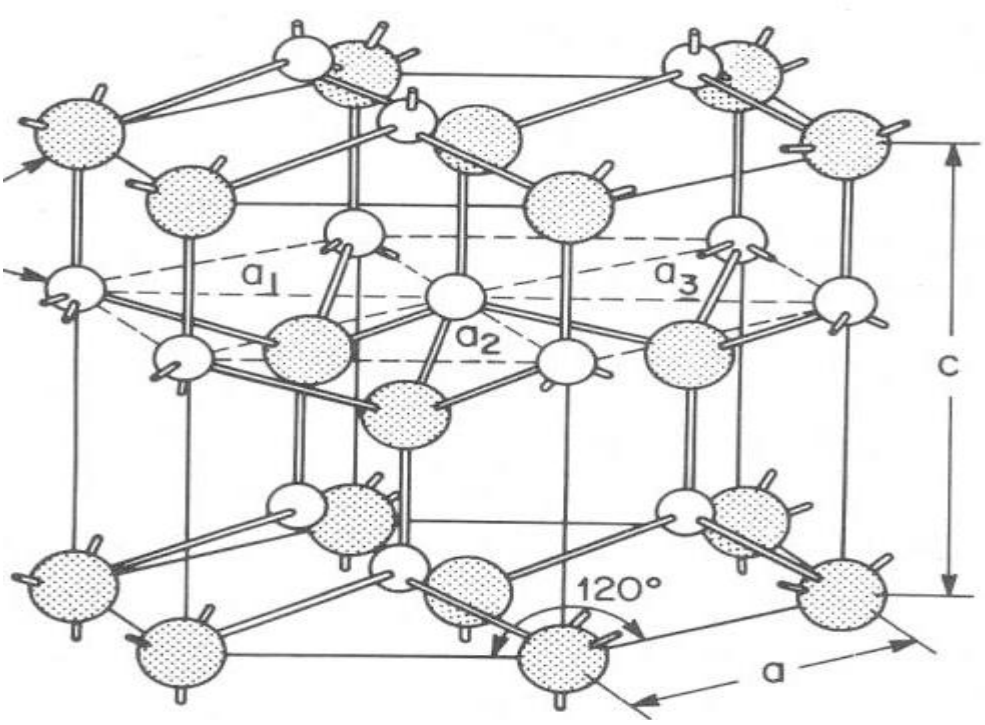

Figure 1.1: Wurtzite crystal structure[11]

1.2 AlGaN/GaN heterostructures Review

AlGaN/GaN based heterostructures have been researched extensively for their use in high temperature, high voltage and high power devices. This is due to their large band discontinuities, larger peak electron velocity, saturation velocity and a higher thermal stability[12- 14] as compared to either Silicon or Gallium Arsenide. Added to these advantages the lack of inversion symmetry leads to a very strong polarization effect in nitride materials [table 1]. Using this property and combining the effects of piezoelectric polarization present due to the strain induced by the lattice and thermal mismatch between AlGaN and GaN, we can achieve a 2 dimensional electron gas density (2DEG) as high as 10^{13} cm^{-2} at the interface without resorting to any intentional doping. In order to achieve this, normally a thin layer of AlGaN is grown on a relatively thick layer of

GaN. For such a wurtzite AlGaN/GaN heterostructure the piezoelectric polarization of the thin AlGaN layer is five times as high as the AlGaAs/GaAs heterostructures. This contributes to a significant increase in the sheet carrier concentration at the interface[15- 16]. Apart from this the spontaneous polarization effect of the group III nitrides in the wurtzite crystal structure is very high. The combination of these two types of polarization leads to a macroscopic electric field responsible for the creation of the interface sheet charge.

Spontaneous Polarization	**AlN**	**GaN**	**InN**
$P_0(Cm^{-2})$	-0.081	-0.029	-0.032

Table 1.1: Spontaneous polarization values of AlN, GaN and InN

1.2.1 Spontaneous and Piezoelectric polarization

Nitrides lack inversion symmetry and exhibit piezoelectric polarization when strained along the [0001] direction[17]. The piezoelectric coefficient of nitrides is almost an order of magnitude higher than the other III-V materials[18]. In GaN a basal surface can be Ga face or N face. It can therefore be either the (0001) face or the (0001) face conventionally representing the Ga face or the N face respectively. These two faces differ in their physical and chemical properties[19].

In the absence of any external electric fields the polarization value (**P)** of AlGaN or GaN is given by

$$P= \mathbf{P_{SP}}+\mathbf{P_{PE}} \text{---------- (1)}$$

Where

$\mathbf{P_{SP}}$= Spontaneous polarization= $P_{SP}\mathbf{z}$

$\mathbf{P_{PE}}$= Strain Induced polarization=$e_{33}\boldsymbol{\varepsilon_z}+e_{31}$ ($\boldsymbol{\varepsilon_x}+\boldsymbol{\varepsilon_y}$)

The relation between $\boldsymbol{\varepsilon_x}$, $\boldsymbol{\varepsilon_y}$ and $\boldsymbol{\varepsilon_z}$ is

$$\boldsymbol{\varepsilon_z}=-2C_{13}/C_{33}(\boldsymbol{\varepsilon_x} \text{ or } \boldsymbol{\varepsilon_y}) \text{ ---------- (2)}$$

Here

C_{13} and C_{33} are elastic constants and e_{33} and e_{31} are piezoelectric coefficients.

Using these equations the piezoelectric polarization is given as,

$$P_{PE}=2(\varepsilon_x \text{ or } \varepsilon_y)\,[e_{31}-e_{33}\,(C_{13}/C_{33})] \text{ ---------- (3)}$$

$[e_{31} - e_{33}\,(C_{13} / C_{33})]< 0$ for AlGaN therefore $P_{PE}< 0$ for tensile and > 0 for compressive strain respectively. The spontaneous polarization of AlN and GaN are both negative[20].

Because of the differences in the structural parameters between GaN and AlN, spontaneous polarization is higher in AlN as compared to GaN. The values of the piezoelectric coefficients and the electric constants are given in Table 2.

Material	**AlN**	**GaN**	**InN**
e_{33}(Cm^{-2})	1.46	0.73	0.97
e_{31}(Cm^{-2})	-0.60	-0.49	-0.57
[e_{31}-e_{33} (C_{13}/C_{33})]	-0.86	-0.68	-0.9

Table 1.2: Piezoelectric coefficients of AlN, GaN and InN

As shown in figure 1.2 piezoelectric and spontaneous polarizations are pointing in the same direction in the case of tensile strain and in the opposite direction in the case of compressive strain. This variation in polarization leads to the creation of a charge density. A 2DEG or a 2DHG will be formed at the interface to compensate for these polarizations induced charges, depending on whether the polarization induced charge is positive or negative. The sheet charge density is a function of the Al content x in $Al_xGa_{1-x}N$ and increase as x increases. For example as x increases from 0.15 to 0.3 the calculated sheet charge density increases from 0.013 to $0.027C/m^2$ [20].

The minimum sheet resistivity for an intentionally undoped AlGaN/GaN with x=0.3 is around 190Ω. Such low values of sheet resistivity combined with thermal stability, high saturation velocity and high sheet carrier concentration make these heterostructures ideal for high power and high frequency applications[20].

At lower frequencies AlGaN/GaN HEMTs are being pursued for power switching applications, biological and chemical sensors.

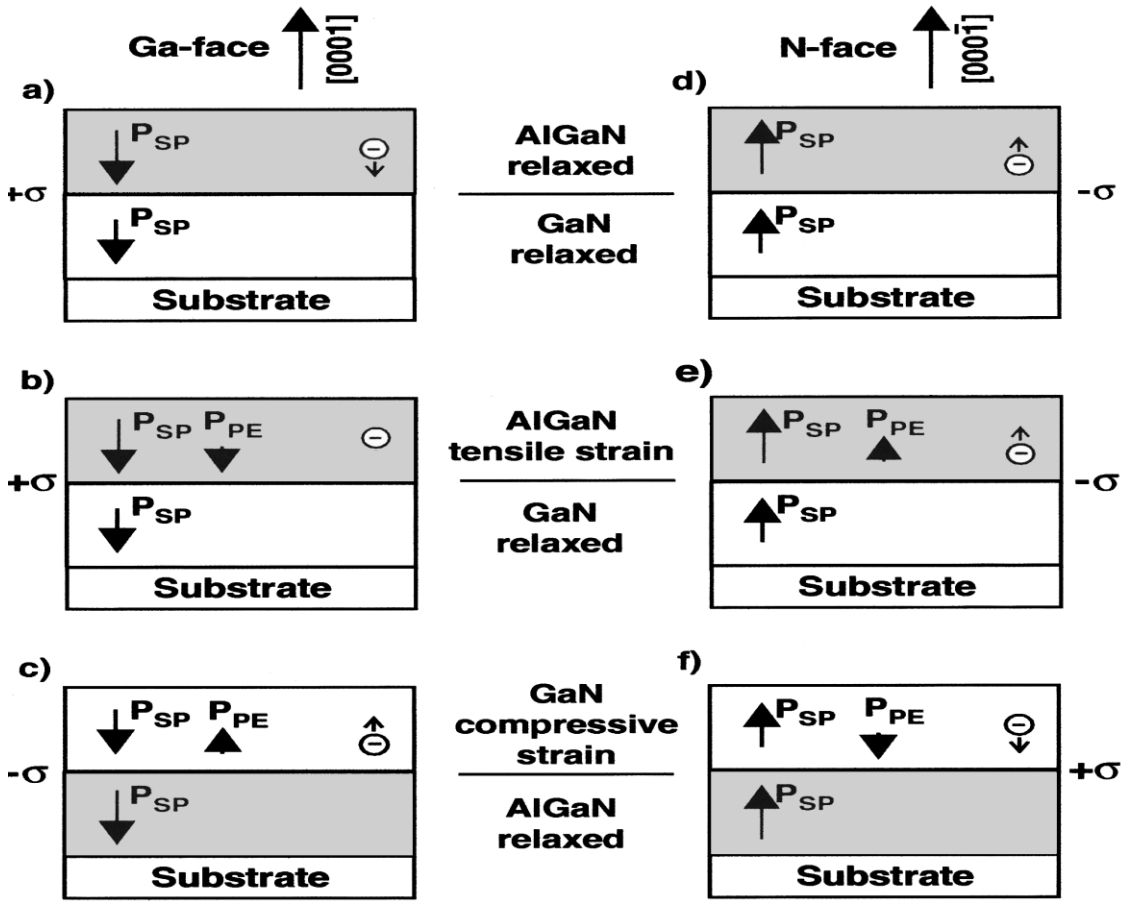

Figure 1.2: Direction of spontaneous and piezoelectric effect in AlGaN/GaN heterostructures

1.3 Introduction to biosensors

A biosensor is an analytical device whose biological sensing element detects the presence of a target analyte and produces an electrical signal in proportion to the analytes concentration[21].

A biosensor can be designed to be sensitive to changes in surface charge density, mass, change in pH, light emission etc. The sensor device can signal this change in the form of a

change in current, potential, mass etc. These sensors can be integrated with electronic devices and this field is broadly called as bioelectronics[22].

1.3.1 DNA and DNA sensors

Watson and Crick described the structure of the DNA in 1953[23]. The DNA is made of repeating units of 4 basic nucleotide bases, adenine, guanine, cytosine and thymine. The DNA is coiled up to form a double stranded helical structure with 2 ss-DNA's held together by hydrogen bonds (Figure 1.3). The structure of the DNA can be maintained single stranded by either applying heat or if it is maintained at a high pH. When these conditions are not maintained 2 ss-DNA's with complementary bases will reanneal to form a dsDNA with adenine pairing with cytosine by 2 hydrogen bonds and guanine with thymine with 3 hydrogen bonds.

In biosensors the probe is an ssDNA sequence, which represents a particular biological species. These sequences are normally between 20-40 bases long. The probe is chosen so that it binds to specific regions from the target probe. Short probes are chosen because they take less time to hybridize but unfortunately they are more prone to nonspecific binding. Another difficulty being that attaching labels to short probes is also difficult. These DNA bases as compared to enzymes or antibodies are stable and easy to synthesize in the laboratory[24-26]. Nucleic acid based probes can also be used to identify genetic mutations or changes in the cellular materials[27].

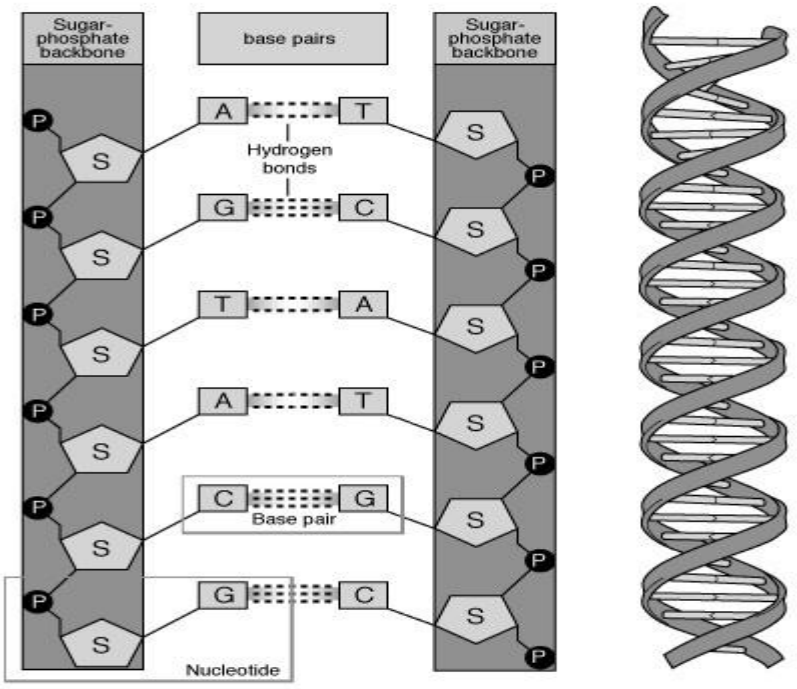

Figure 1.3: Double helix structure of the DNA

1.3.2 Fiber optics

The first biosensor using this method was fabricated by Piunno et al[28]. This type of sensor can detect DNA hybridization in minutes and can be coupled with amplification systems to increase the sensitivities. In this method oligonucleotides (DNA sequences around 20-30 bases long), which are single stranded are used. Here ss-DNA is covalently immobilized onto the quartz optical fiber. The ssDNA can also be synthetically grown on an optical fiber using the well established phosphoromide technology. After this growth the ss-DNA is exposed to its complementary sequence which results in the 2ss DNA's combining to form a double helix. After the DNA hybridization is complete the ds-DNA is exposed to a fluorescent DNA stain Ethidium bromide which attaches itself either to the base stacking region or to the major groove of the double helical structure. The fluorescent intensity, which is proportional to the amount of

cDNA present in the solution, can be monitored using a total internal reflection setup[28]. The device here can also be reused. The sensitivity that can be reached using this method is around 86 ng-ml^{-1} of the complementary DNA. An increase in the fluorescence intensity by almost 200 percent was achieved when the complementary DNA concentration was increased by 100ng-ml^{-1}. The detection time using this method is around 45 minutes[28]. One of the disadvantages of using this method is that ethidium bromide is toxic and until now no proper substitutes for it are available.

1.3.3 Surface Plasmon Resonance

SPR was first successfully demonstrated in 1991 by whitesides et al[29]. The advantage of using surface Plasmon resonance (SPR) technique is that we can measure the kinetics of the bimolecular interactions in real time without using any biomolecular labeling.

Plasma waves can be defined as charge density oscillations propagating in plasma. If these are propagating at the interface of a metal and a dielectric then these are called as surface plasmons (SP). The metal most commonly used is gold because of its chemical inertness and optical properties. The SP is able to exist in this medium because the metal and the dielectric have opposite signs of electric permeability for the wavelength of light being used. The intensity of the SP exponentially decays with distance in a direction normal to the interface. In the SPR technique the propagating vector of the SP matches with the propagating vector of the bulk wave. This resonance is a function of the angle of incidence and hence can be monitored by a graph between reflectance and the angle of incidence. From this graph where the angle of incidence has a minimum in reflectance or a maximum in absorbance we can calculate the refractive index of the boundary media, from which we can calculate the molecules adsorbed on

the metal surface and also the properties of the solution it is in contact with. The SP propagating vector is given as:

$$K_{sp} = K_0 [\varepsilon_m \varepsilon_b / (\varepsilon_m + \varepsilon_b)]^{1/2} \text{---------- (4)}$$

The bulk wave's propagation vector is given as

$$K_b = K_0 \varepsilon_b^{1/2} \text{---------- (5)}$$

Here K_0 is the propagation vector in vacuum.

In order to match these two propagating vectors a prism coupler is used. These prism couplers can be used in two different configurations, Otto [figure 4] or the kretschmann configuration [figure 5]. The kretschamann configuration is the most commonly used configuration for biosensing experiments. In this configuration the plasmons are excited at the surface of the gold film deposited. This setup is now also commercially available.

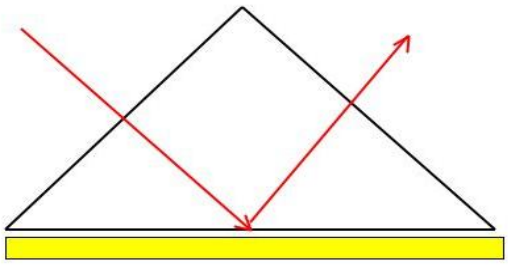

Figure 1.4: Otto configuration

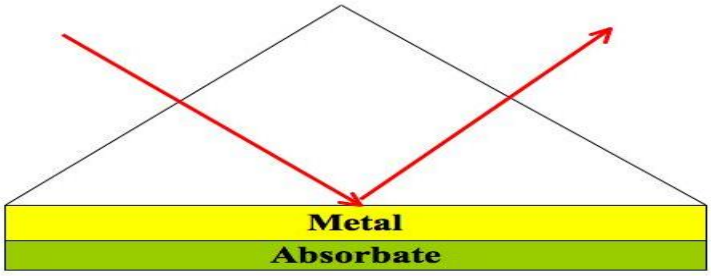

Figure 1.5: Kretschmann configuration

1.3.4 Surface Enhanced Raman spectroscopy (SERS)

Light scattered from a surface consists of two components the elastically scattered Rayleigh light, which is of the same frequency as the incident light and Raman scattered light, which is of different frequency than the incident light. The Raman scattered light can be analyzed to find out the chemical information of the scattering surface. The setup commonly used in a Raman analysis system consists of a laser source, optics to focus the laser source onto the sample surface and detectors to collect the signal. The difficulty in using Raman spectroscopy for analysis is that Raman signal is inherently weak. Statistically only $1X10^{-7}$ of the scattered light is Raman.

This weak Raman signal is enhanced in intensity by a factor of almost 10^8 when it is in proximity or adsorbed onto a metal surface[30-31]. This technique is called as surface enhanced Raman spectroscopy. The advantage of using SERS over the other widely used labeling method like radioactive labeling are non-toxicity, longer shelf life, higher specificity and ease of handling of the SERS probes. The most common SERG probes are silver colloidal particles[32].

1.3.5 Electrochemical methods

Since the 1960's numerous electrochemical methods have been developed for the analysis of nucleic acids. Some of these are cyclic voltammetry, Differential pulse polarography, a.c voltammety etc. In these methods the bare electrode is dipped in a very small volume (3~10μl) of the DNA solution for about 60 seconds. The electrode is then washed with either DI water or buffer solutions. This electrode is then dipped in a blank background electrolyte and the electrochemical measurements are carried out. The electrodes used here are carbon, mercury or gold based electrode. A disadvantage of using mercury based electrodes is that the strong hydrophobic interactions between the bases of the probe DNA and the mercury surface could reduce the DNA hybridization efficiency. The DNA was found not to get properly adsorbed onto the gold based electrodes. But the DNA can be strongly immobilized on gold electrodes when the DNA was thiolated or by using other covalent immobilization procedures.These probes could be used as DNA hybridization sensors. These signals could also be amplified to increase the sensitivity[33- 36].

1.3.6 Piezoelectric transducers

These kinds of transducers use a change in mass to detect a biological event provided this change in mass is greater than the resolution. Some of the advantages are low cost, high

durability and chemical inertness. The material used so far for the construction of a piezoelectric transducer is an AT cut quartz crystal. In this method the resonant frequency of the quartz crystal is maintained by means of an external circuit. When there is a change in mass this is accompanied by a change in frequency which is directly proportional mass change. DNA sequences of a few hundred base pairs can be detected using this method. This can be used to detect both DNA and RNA.

1.4 ISFET's

Silicon is the first material to be used for the fabrication of a FET based sensor that was used in an aqueous medium. These devices were initially called as ISFET's and were used for biomedical applications such as electrophysiological measurements[37].

An ISFET is a modified form of a MOSFET with the gate connection separated from the chip by a reference electrode dipped in an aqueous solution in contact with the gate oxide[38]. Bergeveld used such an ISFET and measured its I_d-V_{ds} characteristics by changing the pH of the aqueous solution to which the gate electrode was exposed. The characteristics obtained were akin to I_d-V_{ds} characteristics of a MOSFET under varying gate voltages[38].

1.4.1 FET based deoxyribonucleic acid (DNA) sensor

The need for a nucleic acids analysis in a fast and reliable manner is generated because of their need in genetics, diagnoses of diseases[39] and in food safety. The commonly used methods like radiolabelling and fluorescence based detection are time consuming and difficult to implement because of the complexities involved in carrying out these reactions and are also difficult to quantify and to transmit the data. A FET based DNA sensor is label free and overcomes some of the above-mentioned problems. The basic mechanism for a FET based

sensor is the DNA hybridization event. In DNA hybridization a probe ssDNA binds with the target DNA, which is also single stranded by forming a dsDNA helix structure with the help of hydrogen bonds. The unique complementary nature of binding between the base pairs namely adenine –thymine and cytosine-guanine is the basis for the DNA hybridization process[40].

In the event of the immobilization of the ssDNA or its hybridization with the complementary ssDNA the charge associated with the DNA alters the electric potential acting on the gate region of the FET. This change in electric potential is reflected as a change in the drain current or the threshold voltage of the FET. DNA is negatively charged in aqueous solutions because of their phosphate background, this charge would affect the charge density in the space charge region of the semiconductor. The change in the current and the detection time has varied depending on the DNA immobilization density[41], immobilization procedure and the buffer solutions used[42-44].

1.5 AlGaN/GaN based biosensors

Initially silicon was used as the material for fabricating semiconductor biosensor. Silicon based FET's had certain drawbacks like lack of chemical stability, need of a reference electrode to apply the bias voltage and the problem of not being able to maintain the activity of the biomolecules on the silicon surface. AlGaN/GaN heterostructures due to their chemical and thermal stability proved to be an excellent substitute for silicon. The chemical stability of GaN ensures that there would be minimum degradation of bio-molecules adsorbed on it. We can also easily integrate this sensor with a GaN based light emitting diode and wireless communication chips.

B. S. Kang et al.[45] used AlGaN/GaN heterostructures to detect DNA hybridization. They used thiolated DNA to tether the DNA molecule to the gold sputtered gate surface. 4% polymethyl methacrylate (PMMA) was used to encapsulate the device except the gate region by e-beam lithography. When the thiol functionalized DNA was exposed to the matching complementary target DNA the DNA hybridization resulted in a change in the source-drain current by 150μA. The same device structure has also been used to detect PSA[46], Kidney injury molecules[47] and glucose[48] at low concentrations by functionalizing the gate surface appropriately.

1.6 References

[1] S. N. Mohammad, Arnel A. Salvador, and Hadis Morkoc, Trans. 1st Int. Hinh Temperature Electron. Conf, Albuquerque, NM, June 1991. "Emerging Gallium Nitride Based Devices"

[2] H. Morkoc, H. Strite, S. Gao, G. B. Lin, M. E. Sverdlov, B. Burns. Appl. Phys. Rev. **76**, 1363 (1994). "A review of large band gap Sic. III-V nitrides, and ZnSe based II-VI semiconductor structures and devices"

[3] B. S. Kang, F. Ren, L. Wang, C. Lofton, Weihong Tan, S. J. Pearton , A. Dabiran, A. Osinsky and P.P. Chow. Appl. Phys. Lett. **87**, 023508 (2005). "Electrical detection of immobilized proteins with ungated AlGaN/GaN high-electron-mobility Transistors"

[4] J. I. Pankove, E. A. Miller and J. E. Berkeyheiser, RCA Rev. **32**, 383 (1971). "GaN electroluminescent diodes"

[5] M. A. Khan, J. M. Van Hove, J. N. Kuznia and D. T. Olsen, Appl. Phys. Lett. **58**, 2408 (1991). "High electron mobility GaN-AlGaN heterostructures grown by LPMOCVD"

[6] S. J. Pearton, F. Ren, A. P. Zhang, K. P. Lee Mater. Sci. Engi. **R30**, 55 (2000). "Fabrication and performance of GaN electronic devices"

[7] H. Morkoc, Nitride semiconductors and devices. New York, Springer, 1999.

[8] H. Amano, N. Sawaki, I. Akasaki and Y. Toyoda, Appl. Phys. Lett. **48**, 353 (1986). "Metalorganic vapor phase epitaxial growth of a high quality GaN film using an AlN buffer layer"

[9] S. Nakamura, Jap. J. Appl. Phys. **30**, L1705 (1991). "GaN Growth Using GaN buffer

layer”

[10] H. Amano, M. Kito, K. Hiramatsu and I. Akasaki, Jap. J. Appl. Phys. **28**, L2112 (1989). “P-type Conduction in Mg-Doped GaN Treated with Low-Energy Electron Beam Irradiation (LEEBI)”

[11]http://kottan-labs.bgsu.edu/teaching/workshop2001/chapter5_files/image018.jpg

[12] R. Wang, C. Young, K. J. Chen, Solid State Electron. **53**, 1 (2006). “Temperature dependence and thermal stability of planar-integrated enhancement/depletion-mode AlGan/GaN HEMTs and digital circuits”

[13] S. Jha, E. V. Jelenkovic, M. M. Pejovic, G. S. Ristic, M. Pejovic, K. Y. Tong, C. Surya, I. Bello, W. J. Zhang, Microelectro. Engineering, **86**, 37 (2009). “Stability of submicron AlGaN/GaN HEMT devices irradiated by gamma rays”

[14] Joachim Piprek, “Nitride Semiconductor devices book” Germany, Wiley-VCH, 2007

[15] A. Bykhovski, B. L. Gelmont, and M. S. Shur, J. Appl. Phys. **81**, 6332 (1997) “Elastic strain relaxation and piezoeffect in GaN-AlN, GaN-AlGaN and GaN-InGaN superlattices”

[16] E. T. Yu, G. J. Sullivan, P. M. Asbeck, C. D. Wang, D. Qiao, and S. S. Lau, Appl. Phys. Lett. **71**, 2794 (1997) “Measurement of Piezoelectrically Induced Charge in GaN/AlGaN Heterostructure Field-Effect Transistors”

[17] P. Lawaetz, Phys. Rev. B **5**, 4039 (1972) “Study of Wurtzite structures”

[18] A. Bykhovski, B. L. Gelmont, and M. S. Shur, J. Appl. Phys. **81**, 6332 (1997). “Elastic strain relaxation and piezoeffect in GaN-AlN, GaN-AlGaN and GaN-InGaN superlattices”

[19] E. S. Hellman, MRS Internet J. Nitride Semicond. Res. **3**, 11 (1998)

[20] O. Ambacher, J. Smart, J. R. Shealy, N. G. Weimann, K. Chu, M. Murphy, W. J. Schaff, L. F. Eastman, R. Dimitrov, L. Wittmer, M. Stutzmann, W. Rieger and J. Hilsenbeck, J. Appl. Phys. **85**, (1999). "Two-dimensional electron gases induced by spontaneous and piezoelectric polarization charges in N- and Ga-face AlGaN/GaN heterostructures"

[21] Z. Junhui, C. Hong and Y. Ruifu DNA based biosensors, biotech. Advances, **15**, 43, (1997). "DNA based biosensors"

[22] I. Willner, E. Katz, Bioelectronics an Introduction. Wiley-VCH, 2005.

[23] J. D. Watson and F. H. C. Crick. Nature (1953). "Genetical implications of the structure of deoxyribonucleic acid"

[24] F. V. Bright, T. A. Betts, K. S. Litwiler, Anal. Chem. **62**, 1065 (1990).

[25]Vo-Dinh, T.; Griffin, G. D. Sepaniak. M. J. In Fiber Optic Chemical Sensors and Biosensors; Wolfbeis, 0. S., Ed.; CRC Press: Boca Raton, FL, 1991.

[26] K. M. Shokat, P. G. Schultz, Methods Enzymol. 1993, 203, 327-351.

[27] F. E. Young JAMA, **229**, 2404 (1987). "DNA probes: fruits of the new biotechnology"

[28] P. A. E. Piunno, U. J. Krull, R. H. E. Hudson, M. J. Damha and H. Cohen, Anal. Chem. **67**, 2635 (1995). "Fiber-optic DNA sensor for fluorometric nucleic acid determination"

[29] K. L. Prime and G. M. Whitendes, Science, **252**, 1164 (1991). "Self-Assembled Organic Monolayers: Model Systems for Studying Adsorption of Proteins at Surfaces"

[30] D. J. Jeanmarie, R. P. Van Duyne, J. Electroanal. Chem. **84**, 1 (1977). "Surface Raman spectroelectrochemistry: Part I. Heterocyclic, aromatic, and aliphatic amines adsorbed on the anodized silver electrode"

[31] V. O. Dinh, T. Houck, K. Stokes, Anal. Chem., **66**, 3379 (1994). "Surface Enhanced Raman gene probes"

[32] M. H. Chowdhury, B. Atkinson, T. Good, Proceedings of SPIE, **4965**, 111 (2003). "Surface enhanced Raman spectroscopy for the detection of pathogenic DNA and protein in foods"

[33] I. Willner, E. Katz, Bioelectronics an Introduction. Wiley-VCH, 2005.

[34] F. Patolsky, A. Lichtenstein, I. Willner, J. Am. Chem. Soc. **123**, 5194 (2001). "Electronic Transduction of DNA Sensing Processes on Surfaces: Amplification of DNA Detection and Analysis of Single-Base Mismatches by Tagged Liposomes"

[35] F. Patolsky, E. Katz, A. Bardea, I. Willner, Langmuir, **15**, 3703 (1999). "Enzyme-Linked Amplified Electrochemical Sensing of Oligonucleotide-DNA Interactions by Means of the Precipitation of an Insoluble Product and Using Impedance Spectroscopy"

[36] V. Vetteri, N. Papadopoulos, V. Drazan, L. Strasak, S. Hason, J. Dvorak, Electrochim. Acta. **45**, 2961 (2000). "Sensitive detection of cyclophosphamide using DNA-modified carbon paste, pencil graphite and hanging mercury drop electrodes"

[37] K. D. Wise, J. B. Angell, A. Starr, IEEE Trans. Biomed. Eng. **17**, 238 (1970). "An integrated-circuit approach to extracellular microelectrodes"

[38] P. Bergveld, Sens. Actuators, **88**, 1 (2003). "Thirty years of ISFETOLOGY: What happened in the past 30 years and what may happen in the next 30 years"

[39] C.H. Mastrangelo, P. Vincenzini, L. Dori, Techna, Faenza, 1999.

[40] Poghossian, A. Cherstvy, S. Ingebrandt, A. Offenhausser, M.J. Schoning, Sens. Actuators, **111**, 470 (2004). "Possibilities and limitations of label-free detection of DNA hybridization with field-effect-based devices"

[41] D. S. Kim, Y. T. Jeong, H. K. Lyu, H. J. Park, J. K. Shin, P. Choi, J. H. Lee, G. Lim, Biosens. Bioelectron. **20**, 69 (2004). "An FET-type charge sensor for highly sensitive detection of DNA sequence"

[42] F. K. Perkins, L. M. Tender, S. J. Fertig, M. C. Peckerar, Proc. SPIE. **4608**, 251 (2002). "Sensing macromolecules with microelectronics"

[43] F. Wei, B. Sun, Y. Guo, X. S. Zhao, Biosens. Bioelectron. **18**, 1157 (2003). "Monitoring DNA hybridization on alkyl modified silicon surface through capacitance measurement"

[44] D. S. Kim, Y. T. Jeong, H. K. Lyu, H. J. Park, H. S. Kim, J. K. Shin, P. Choi, J. H. Lee, G. Lim, M. Ishida, Jpn. J. Appl. Phys. **42**, 4111 (2003). "Fabrication and characteristics of a field-effect transistor-type charge sensor for detecting deoxyribonucleic acid sequence"

[45] B. S. Kang, S. J. Pearton J. J. Chen , F. Ren, J. W. Johnson, R. J. Therrien, P. Rajagopal, J. C. Roberts, E. L. Piner, and K. J. Linthicum, Appl. Phys. Lett. **89**, 122102 (2006). "Electrical detection of deoxyribonucleic acid hybridization with AlGaN/GaN high electron mobility transistors"

[46] B. S. Kang, H. T. Wang, T. P. Lele, Y. Tseng, F. Ren, S. J. Pearton, J. W. Johnson, P. Rajagopal, J. C. Roberts, E. L. Piner, and K. J. Linthicum, Appl. Phys. Lett. **91**, 112106 (2007). "Prostate specific antigen detection using AlGaN/GaN high electron mobility transistors"

[47] H. T. Wang, B. S. Kang, F. Ren, S. J. Pearton, J. W. Johnson, P. Rajagopal, J. C. Roberts, E. L. Piner, and K. J. Linthicum, Appl. Phys. Lett. **91**, 1222101 (2007). "Electrical detection of kidney injury molecule-1 with AlGaN/GaN high electron mobility transistors"

[48] B. H. Chu, B. S. Kang, S. C. Hung, K. H. Chen, F. Ren, A. Sciullo, B. P. Gila, S. J. Pearton, J Diabetes Sci Technol. **4**, 171 (2010). "Aluminum gallium nitride (GaN)/GaN high electron mobility transistor-based sensors for glucose detection in exhaled breath condensate"

CHAPTER 2

Device Processing

2.1 Wafer Dicing

The AlGaN/GaN HEMT is purchased from SWT Associates. The HEMT structure consists of a thin AlN layer, 2.7µm GaN buffer, 20nm AlGaN layer and a 2nm GaN cap layer. The GaN cap layer reduces the surface states and improves the ohmic source and drain contacts without having any ill effects on the schottky contact[1, 2]. The epilayers are grown on top of sapphire. The 2 dimensional electron gas (2DEG) electron mobility is greater than 1300cm^2/v-s. The wafer is diced using a hubbed resinoid blade. The 2" wafer is diced into individual pieces of dimensions 5mm X 5mm. The wafer is cut from the sapphire side.

2.2 Cleaning

The 5mm X 5mm wafer pieces are cleaned in the solvents in the following order: Acetone, trichloroethylene, Acetone, methanol and again in methanol. The cleaning is done for a period of 5 minutes in each solvent using an ultrasonicator. After this the sample is heated at 100^{o}C for 10 minutes in a solution containing a mixture of Hydrochloric acid (HCl) and water present in the ratio of 1:1 by volume.

This cleaning step is used to remove the native oxides present on GaN. It was demonstrated that dissolving HCl in water results in a cleaner surfaces than dissolving HCl in methanol[1]. An HCl: DI

water solution is also found to produce the lowest C/N ratio[2] and increase the Chlorine (Cl) concentration on the surface. These Cl contaminants might be useful since they have been found to improve the adhesion of metals like Au, Ag, Ni, Pd, and Pt to the surface[3, 4]. Finally the sample is rinsed in DI water. The sample is examined under an optical microscope to verify if the surface has been successfully cleaned. If not, the samples are cleaned a second time for a period of 5minutes in acetone, methanol and DI water. There is however no standard protocol for surface cleaning before depositing the contacts. The cleaning procedure has to be optimized depending on the following processing steps and the final goal.

Figure 2.1: Sample cleaning station

2.3 Photolithography

Photolithography is the process of transferring the geometrical patterns from the mask to the substrate. Photolithography is the most important step during device processing since this step defines the device dimensions, resolution that can be achieved and the throughput of the process. In this process the substrate is first coated with a radiation sensitive polymer known as photoresist. The thickness of the coated film is dependent on the rotational speed of the spin coater, the time of rotation and the viscosity of the polymer. A soft bake step is next performed where the resist coated substrate is baked in an oven at 100^{0}C for a period of 60~120 seconds. This step is done to evaporate the solvents in which polymer is dissolved. The photoresist is then exposed to the UV radiation either with or without a mask. The parts of the resist that are exposed to the radiation either soften or harden depending on whether a positive or a negative photoreisist is used respectively. The substrate is then exposed to a developing solution. On exposure to the developing solution either the exposed or the unexposed regions of the photoresist wash away depending on whether we are using a positive or a negative photoresist. In case of a positive photoresist the pattern on the mask and the substrate are the same and in case of a negative photoresist the pattern on the substrate is the negative of the pattern on the mask.

A negative photoresist has two constituents a polymer and a photosensitive compound. The photosensitive compound gets activated when exposed to radiation and transfers this energy to the polymer. The polymer on absorbing this energy cross-links and its molecular weight increases. Due to this increase in molecular weight they become more difficult to dissolve in the developer solution. When using a negative photoresist the resolution will be relatively poor because the unexposed parts share a tendency to swell when exposed to the developer solution. A positive photoresist consists of a base resin and a photosensitive compound. This photosensitive

material becomes soluble only after exposure to the radiation. In a positive photoresist there is no problem of swelling unlike the negative photoresist. The disadvantage of using a positive photoresist is bad throughput as compared to the negative photoresist. Positive photoresists have bad throughput since we have to ensure that all of the photosensitive material is exposed to enough time to so that it can be completely dissolved. These exposures are normally carried out in nitrogen ambient since oxygen has a cross-linking inhibition action. This is especially necessary when using a negative photoresist. In case lift off is one of the processing steps then the photoresist that is commonly used is the image reversal photoresist, since a liftoff procedure calls for a negative wall profile[4].

For depositing the protective mask during device isolation or during the ohmic and Schottky contact metallization the following procedure is used. The 5mm X 5mm AlGaN/GaN HEMT wafer is attached to a 4" silicon wafer using silver paint. This is done for the purpose of spin coating and photolithography. Shipley AZ5214E, the image reversal photoresist is then spin coated at a speed of 4000 rotations per minute for a period of 30 seconds. A soft bake step is then performed at 100^{0}C for 60 seconds. The wafer is then exposed to UV radiation for 30 seconds through a mask. After this the thermal curing is performed at a temperature of 110^{0}C for 60 seconds. Following the thermal curing a flood exposure step is carried out for a period of 60 seconds. The pattern is then exposed to the developer solution for a period of about 120~150seconds and then rinsed with DI water and then blown dry with nitrogen.

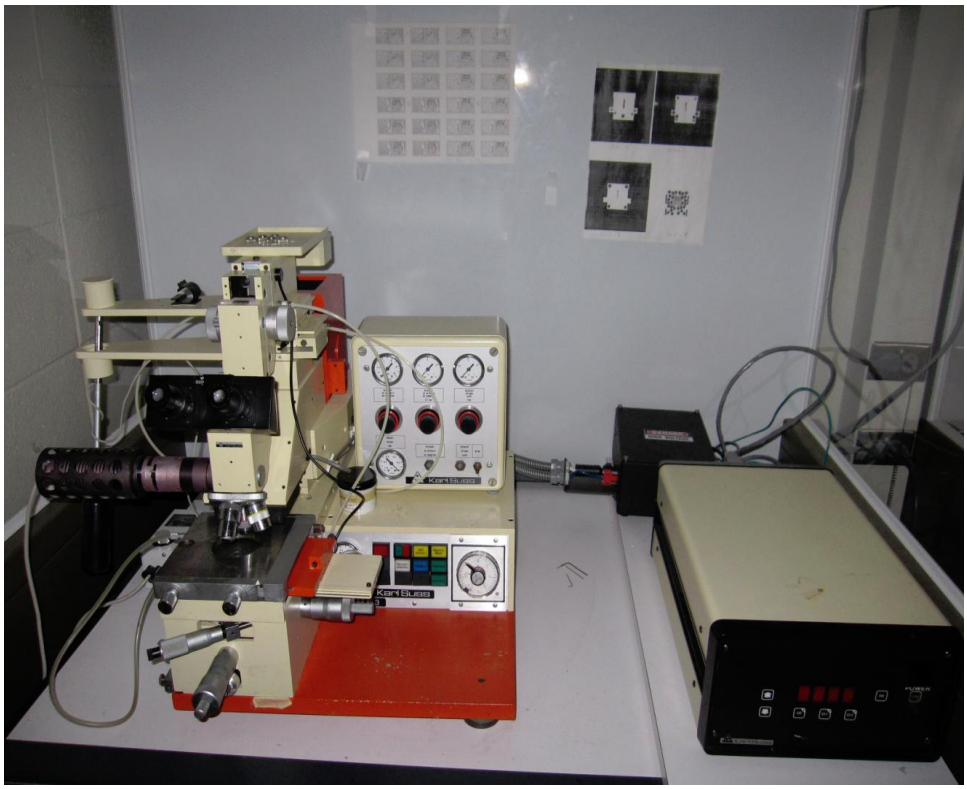

Figure 2.2: Photolithography system

2.4 Reactive Ion etching

Reactive Ion Etching (RIE) or dry etching is preferred in semiconductor processing as compared to wet etching as it is easier to automate and is also anisotropic in nature, hence the problem of undercutting is avoided. It is also easier to vent the corrosive gases as compared to wet etching. Apart from these advantages the additional advantage of using a plasma etching system is that we can achieve reactions, which are only possible at high temperatures at a lower temperature ambience. This is possible because the equivalent temperature of the electrons is very high because of the inefficient energy transfer mechanism between the electrons and the ions. A basic plasma reactor consists of two parallel electrodes, which are kept at low pressure. A high frequency RF voltage is applied between these two electrodes. Now when the plasma starts, the electrons diffuse faster to the chamber walls because of there lower mass as compared to the positive ions, which are concentrated at the centre. Hence the region between these two ions is depleted of any charge carriers. Due to the applied RF voltage to the electrodes the electrons are attracted to the momentarily positive electrode and the electrons easily move towards the positive electrode. The negative electrode attracts the ions, which are slow to move. Hence between the positive electrode and the ions a high potential develops which determines the energy of ion bombardment on any material placed on the cathode.

GaN is chemically very stable and hence dry etching is the dominant technique. RIE is performed using a 13.65 MHz RF power supply, RFX-600 and an impedance-matching unit ATX-600. In order to have a planar process NF_3 based plasma chemistry was used to achieve device isolation. The incorporation of fluorine ions into the AlGaN and the GaN layers can deplete the 2DEG gas from the active channel and provide device isolation. The device isolation achieved by this method was proved to be as good as the isolation achieved by using Cl_2/Ar plasma[7]. Mo/Ni is

used as the protective mask for the NF_3 plasma. The dry etching is carried out at a NF_3 flow rate of 9 sccm at a power of 20 watts for a period of 1200 seconds. After the etching molybdenum is etched off by using hydrogen peroxide and the wafer is cleaned in Acetone, methanol and DI water for a period of 5 minutes using an ultrasonicator.

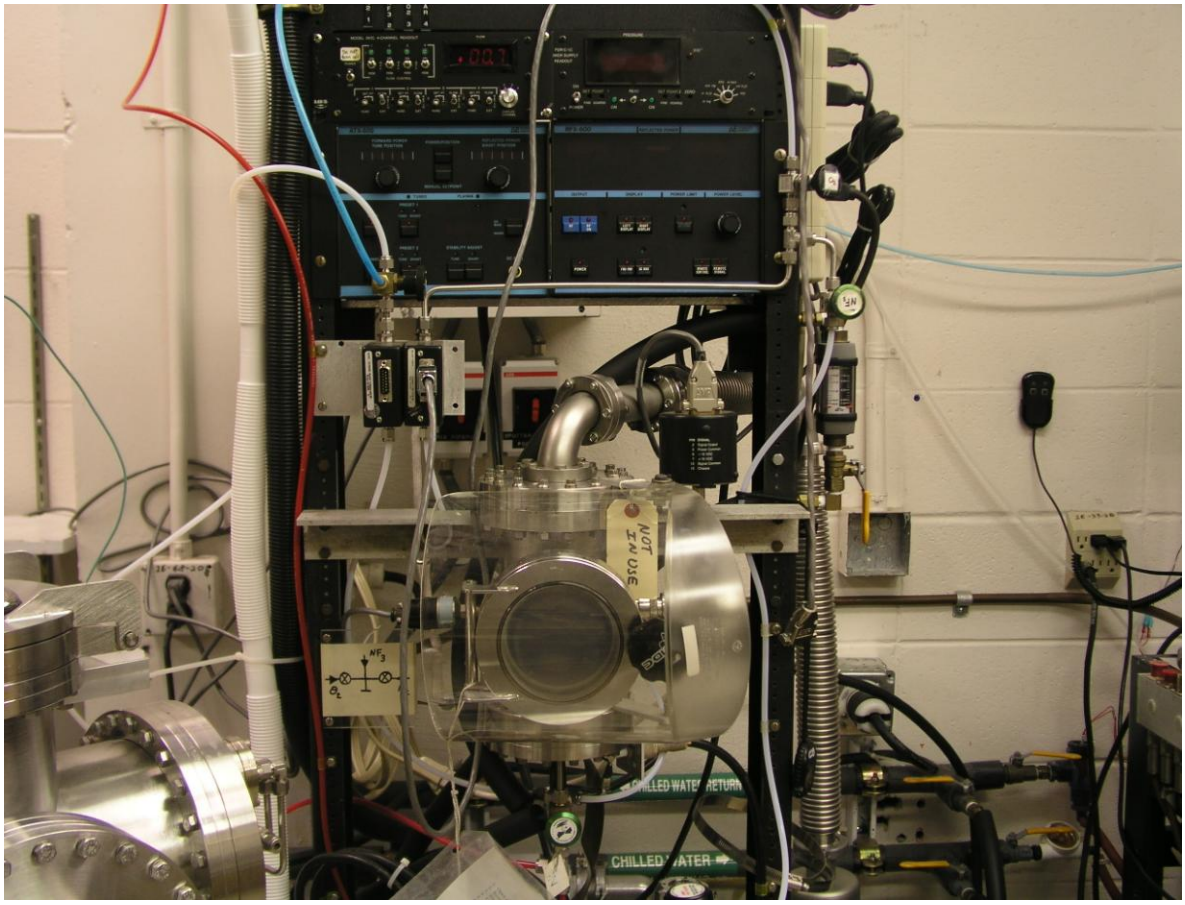

Figure 2.3: Reactive ion etching system

2.5 Sputtering

Due to GaN's wide band gap of 3.4 eV, it is difficult to fabricate good low resistance ohmic contacts. Ti containing metallization schemes are the most widely used ohmic contacts. The bonding between Gallium and Nitrogen in GaN is very strong and is equal to 8.92ev/atom[8]. The bonding between Titanium(Ti) and Nitrogen(N) in Titanium nitride(TiN) is also very strong. So when Ti is alloyed with GaN there is a competitive reaction between Ti and Ga for the N atom. But since TiN has a higher enthalpy of formation, TiN is formed which leads to a nitrogen vacancy in GaN which acts as a donor site. This increases the electron concentration and hence makes GaN highly n type and leads to the formation of low contact resistance ohmic contacts[9, 10]. In order to prevent the out diffusion of Ga atoms a very thick layer of Al (200nm) is sputtered on top of Ti. Ti also has the ability to penetrate any insulating surface oxide if it is present on the surface[11]. This property is responsible for creating low resistance contacts. Both Ti and Al have a tendency to get oxidized very easily and thereby increase the contact resistance. To prevent this Au is sputtered. Ni and Cr are sputtered between Al and Au to prevent the formation of any intermetallic compounds between Au and Al during annealing and to increase the adhesion of Au to Ni. Au also serves as the electrical contact. These metallizations are annealed between 750^{0}C and 900^{0}C for the ohmic contact formation. Since Al has a relatively low melting of around 660^{0}C it has a tendency to "ball up" during annealing. Ni on top of Al prevents this from happening and hence also maintains a smooth morphology[12]. The addition of Ni and Au is not necessary for the performance of the contact in the short term but are very necessary for device applications. Since the ohmic contacts that we are fabricating need to have low contact resistance and also be able to provide smooth surface for gold wire bonding, the following metallization scheme was developed. Ti (40nm)/Al (200nm)/Ni (40nm) were sputtered by DC magnetron

sputtering system. After lift off these contacts were annealed in nitrogen overpressure for 30 seconds at 750^{0}C. Following this a very thin layer of chromium and gold were sputtered. Of all the various metallization schemes tried (Table 2.1) this procedure gave us durable gold contacts.

Serial no.	Order of depositing ohmic contacts	Annealing Temperature in N_2 atmosphere	Durability of gold wire bonding
1	Ti/Al/Ni/Au	750	Ok
8	Ti/Al/Ni/Au	850	Ok
9	Ti/Al +annealing+Ni/Au	750	Bad
4	Ti/Al +annealing+Ni/Au	850	Bad
5	Ti/Al/Ti/Au	750	Bad
6	Ti/Al/Ti/Au	850	Bad
7	Ti/Al+Annealing+Ti/Au	750	Bad
8	Ti/Al+Annealing+Ti/Au	850	Bad
9	Ti/Al/Ni+Annealing+Cr/Au	750	Good

Table 2.1: Durability of gold wire bonding to ohmic contacts

Figure 2.4: Interior of the sputtering system

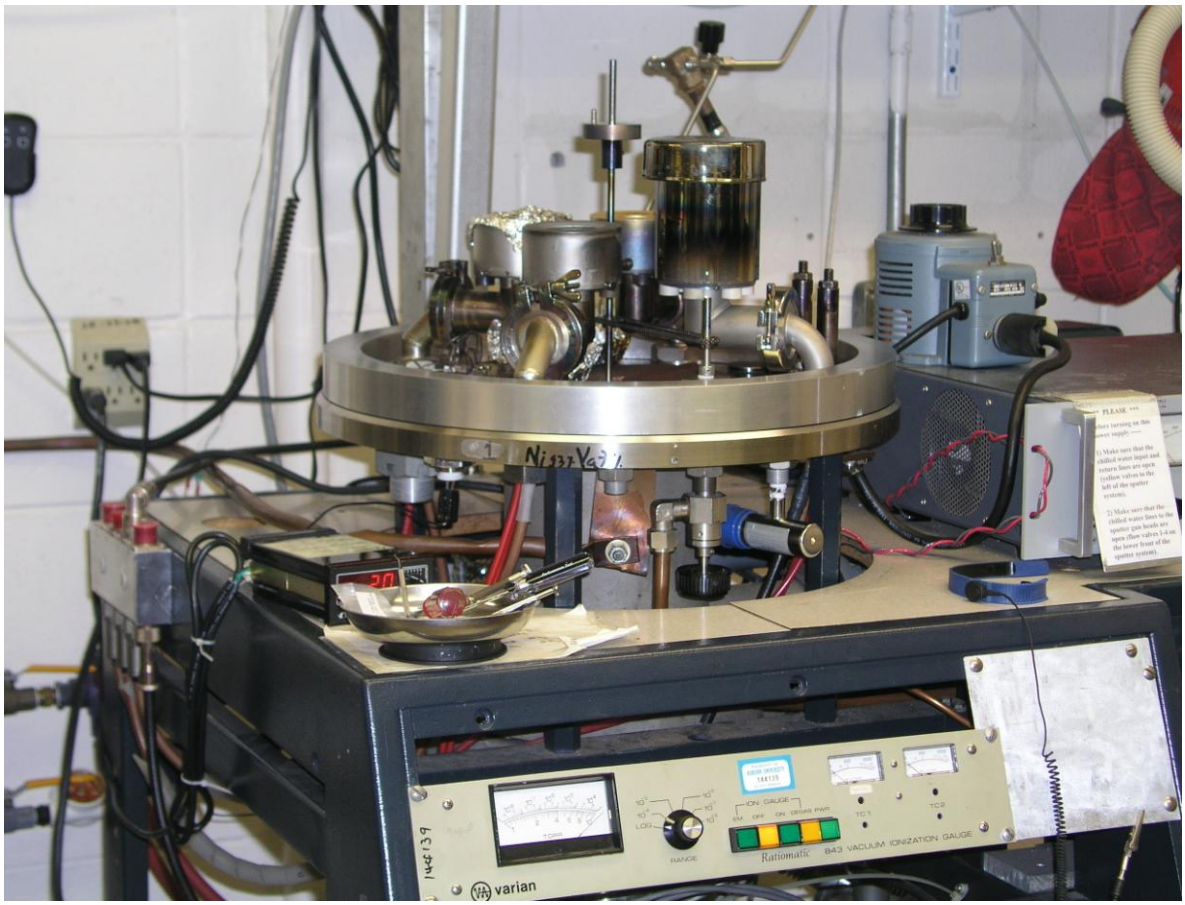

Figure 2.5: Exterior of the sputtering system

2.6 Lift-off

Liftoff is the procedure that is used to pattern metal films on a substrate. Initially the pattern is defined on the substrate by photoresist. Since the photoresist is spin coated onto the substrate patterns are normally avoided at the edges of the substrate due to the edge bead effect. By the process of sputtering, the metal is deposited all over the substrate patterned with the photoresist. The photoresist should not get overheated during sputtering, since this could cause trouble with liftoff. The substrate is then exposed to acetone. Acetone is a solvent for the photoresist. Acetone in the process of dissolving the photoresist also removes the metal deposited on top of it. After this the substrate is then washed with methanol and DI water and blown dry with nitrogen. Drying the sample should be avoided until all the metal from the desired locations are removed.

2.7 Rapid Thermal Annealing

Rapid thermal annealing is performed so that Ti can react with GaN to form TiN which generates nitrogen vacancies that makes the surface highly n-type. The 5mm X 5mm sample is kept at the centre of the carbon strip. An optical pyrometer focused near the sample on the carbon strip is used to record the temperature. The chamber is pumped to a pressure of $4X10^{-7}$ torr. 99% pure N_2 is then passed inside the chamber for a period of 15 minutes. The temperature is ramped up to 750^{0}C and maintained for 30 seconds. After the 30 seconds the temperature is immediately brought down to room temperature.

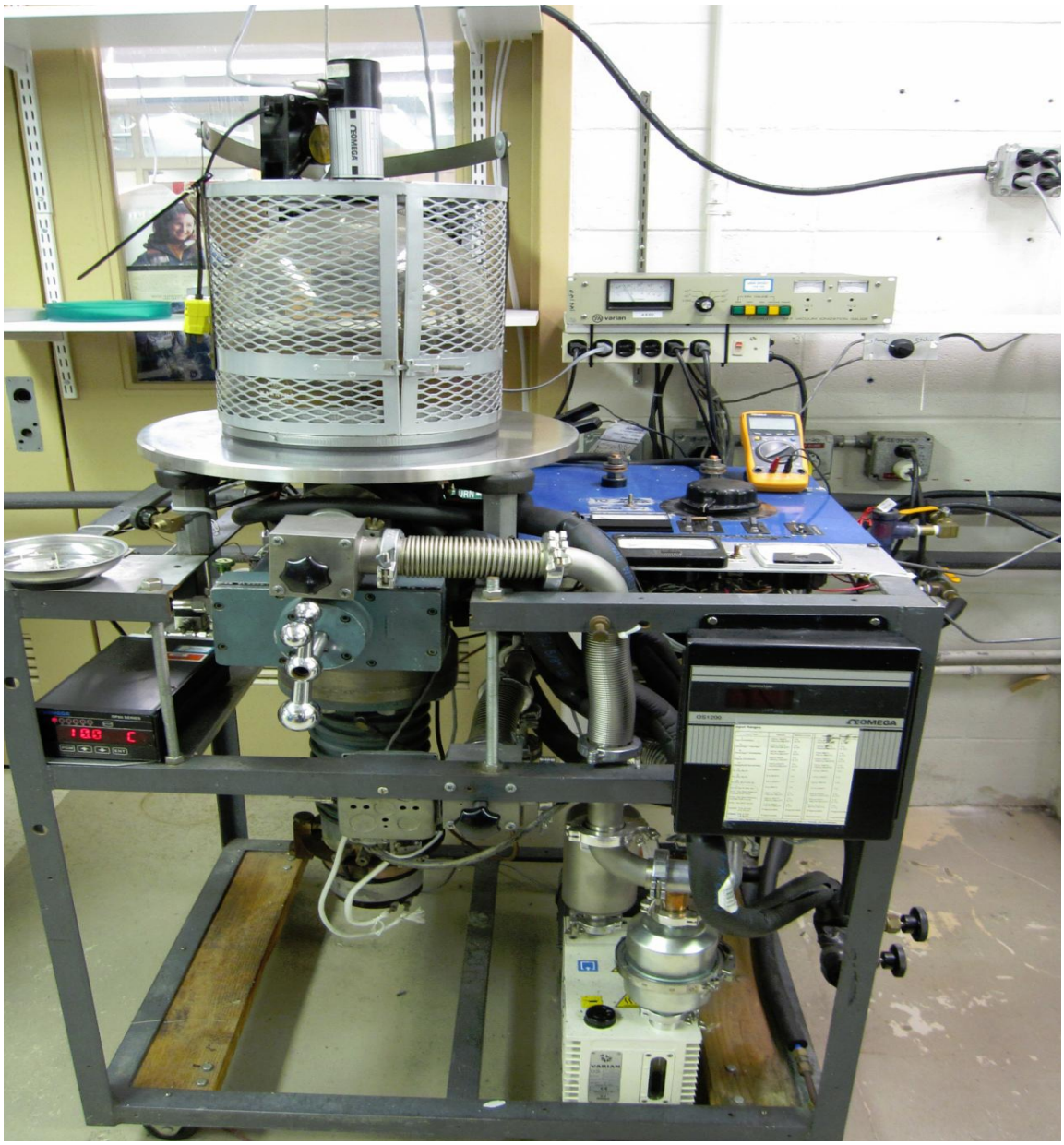

Figure 2.6: Rapid thermal annealing system

2.8 Device Encapsulation

The FET Device needs to be operated in a liquid environment. The liquid environment may be acidic or basic in nature. For this the device needs to be encapsulated with an insulating and a chemically stable material. A poor encapsulating medium will lead to an unstable device. A good encapsulation also ensures device reusability. Some of the common encapsulates that have been used are epoxies, SU-8[13], SiO_2[14] and PDMS[15].

PDMS or polydimethylsiloxane is a silicone elastomer, which has gained popularity for use in microfluidic fabrications and as an encapsulant. The advantages of PDMS are twofold, it is inexpensive and is a silicone material, that is easy to process. PDMS is chemically inert, not permeable to liquids, thermally stable and being transparent it is also easy to optically align on a substrate.

Some of the common methods used to pattern PDMS on a device include making predefined PDMS molds and then aligning them on the substrate[16], patterning PDMS using an combination of photolithography, sputtering and dry etching[17] and adding photoinitators to PDMS to make it photodefinable[18].

In case of the AlGaN/GaN HEMT based biosensor PDMS is used to encapsulate the entire device except the gate region. The gate region is then biofunctionalized for the purpose of biosensing.

A dry etching process to pattern PDMS on the FET is developed using standard fabrication methods and etch gases. PDMS from Dow corning is mixed with the curing agent in the ratio of 10:1 by weight. The mixture is mixed and then pumped to remove any bubbles formed during the mixing. The mixture is then spin coated on the device. The device is exposed to oxygen plasma

for a period of 1800 seconds at a power of 20 watts. The oxygen flow rate is set at 20 Sccm. This process is necessary since PDMS is hydrophobic. Due to hydrophobic nature of PDMS, Photolithographic patterning is very difficult on the device. Exposure to an oxygen plasma increases the surface activation energy of PDMS and hence also its wetabillity. After this process the photoresist is spin coated on the PDMS. The source and drain mask is used to pattern the photoresist on PDMS. The photolithography step has to be performed immediately after the oxygen plasma exposure, since the surface recovers its natural hydrophobic state over time. High purity Molybdenum (MO) and Nickel- Vanadium ($NiV_{7\%}$) are sputtered. A liftoff procedure is carried out after the sputtering.

Unlike ordinary polymers, which can be etched using oxygen plasma, PDMS being a silicone polymer requires a different etch chemistry to break the siloxane (Si-O) bonds. A fluorine based etch chemistry is used to etch PDMS similar to the etch chemistry of SiO_2. Hence a NF_3 plasma is used to etch PDMS. The PDMS is exposed to the fluorine plasma for a period of 90 minutes at a flow rate of 30 Sccm.

The etching is carried out at a power of 30 watts. The etching is determined to be approximately 11µm/hr using a profilometer. After etching the PDMS , Mo is etched away using hydrogen peroxide. Along with Mo the Ni on top of it is also etched off.

The disadvantages of using dry etching for PDMS is in determining the etch stop. An under etched or an over etched surface can result in difficulties with the biofunctionalization of DNA on the gold surface. Hence an alternative approach was used was to encapsulate the device by using photodefinable PDMS. PDMS can be made photodefinable by adding photoinitiators to it. Photodefianble PDMS, WL-5150 from DOW corning is used to encapsulate the device. WL-5150 is a silicone elastomer, which can be photopatterned using standard lithography processes.

The silicone material is prepared in mesitylene with a solution viscosity of 450cP. The solution is stored at a temperature of -15^{0}C. Prior to use it is equilibrated to room temperature. The following steps were followed to photopattern the PDMS.

2.8.1 Spin coating process:

The device is cleaned in acetone, methanol and DI water to remove any surface impurities. Around 10ml of the photodefinable PDMS is pippeted onto the device. Initially the spin coater is spun at 500rpm for 10seconds. This allows to solution to uniformly spread around the device. After this the spin coater is operated at 1500rpm for 30seconds.

2.8.2 Soft bake

In order to remove the residual solvent the wafer is now baked at a horizontal or flat position at 110^{0}C for 4 minutes in an oven. The horizontal position is maintained in order to prevent any downward flow of PDMS. Even after this bake the PDMS surface remains tacky.

2.8.3 UV exposure

PDMS now needs to be exposed to UV light in order to activate the photosensitive compound. Activation of the photosensitive compound results in the selective cross-linking of the exposed regions during the hard bake step. The surface is exposed to 160mJ/cm^{2} of UV light for a period of 5 minutes.

2.8.4 Post exposure bake

This bake is necessary to make the exposed parts insoluble in the developing solution. The PDMS is now baked at 150^{0}C for a period of 90 seconds.

2.8.5 Development

The wafer is now developed in a developing solution for a period of 2~3minutes. After the development it is blown dry with N_2 gas.

2.8.6 Hard bake

The developed wafer is now hard baked in an Oven at 110^0C for 30 minutes. This process is performed to maximize the cure level and the mechanical properties.

2.8.7 Lithographic process performance

After hard baking the device, the thickness of the photodefianble PDMS layer is measured. The thickness is measured to be around 20μm.

2.9 I-V characteristics

Figure 2.7 and Figure 2.8 Show the I_{ds}-V_{ds} and the gate leakage characteristics of the device respectively, after the above mentioned device processing steps are carried out. Figure 2.7 demonstrates the effectiveness of the fluorine plasma isolation. As seen in Figure 2.8 the gate leakage current is very low for the drain-source voltage and the gate bias, for the voltage range where the device is used as a biosensor.

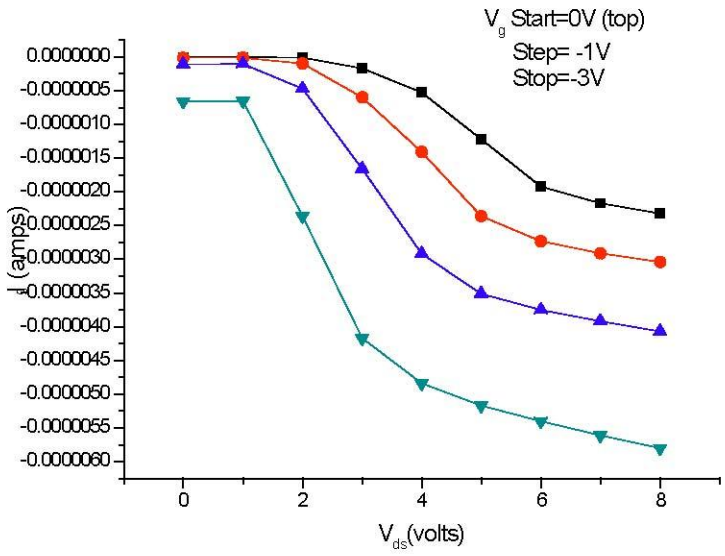

Figure 2.7: I_{ds}-V_{ds} characteristics of the device

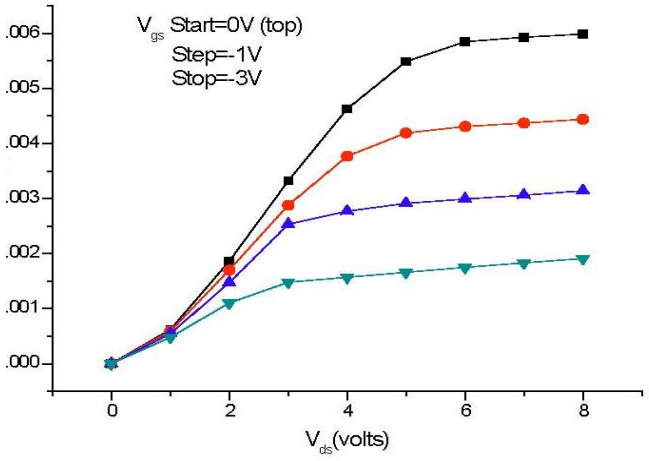

Figure 2.8: I_g-V_{ds} characteristics of the device

2.10 References

[1] D. H. Kim, V. Kumar, G. Chen, A. M. Dabiran, A. M. Wowchak, A. Osinsky and I. Adesida, Electron. Lett. **43**, 127 (2007). "ALD Al_2O_3 passivated MBE-grown AlGaN/GaN HEMTs on 6H-SiC"

[2] A. Kuliev, V. Kumar, R. Schwindt, D. Selvanathan, A. M. Dabiran, P. Chow, I. Adesida, Solid State Electron. **47**, 117 (2003). "0.15 μm gate-length AlGaN/GaN HEMTs with varying gate recess length"

[3] L. L. Smith, S. W. King, R. J. Nemanich, R. F. Davis, J. Electron. Mater. **25**, 805 (1996). "Cleaning of GaN Surfaces"

[4] M. Dialea, F. D. Aureta, N. G. Van der Berga, R. Q. Odendaala, W. D. Roosb, Appl. Surf. Sci. **246**, 279 (2005). "Analysis of GaN cleaning procedure"

[5] I. Shalish, Y. Shapira, L. Burstein and J. Salzan, J. Appl. Phys. **89,** 390 (2001). "Surface states and Surface oxide in GaN layers"

[6] http://groups.mrl.uiuc.edu/dvh/pdf/AZ5214E.pdf

[7] R. Wang, Y. Cai, C. W. Tang, K. M. Lau and K. J. Chen, Jpn. J. Appl. Phys. **46**, 2330 (2007). "Device isolation by plasma treatment for planar integration of enhancement/depletion-mode AlGaN/GaN high electron mobility transistors"

[8] A. J. Steckl, I. Chyr, J. Vac. Sci. Technol. B **17**, 362 (1999). "Focussed ion beam milling of GaN and related substrate materials (Sapphire, SiC and Si)"

[9] F. Rahman, S. Xu, I. M. Watson, D. K. B. Mutha, R. K. Oxland, N. P. Johnson, A. Banerjee and

E. Wasige, Appl. Phys. A, **94**, 2008 (633). "Ohmic contact formation to bulk and heterostructure gallium nitride family semiconductors"

[10] W. Y. Uen, Z. Y. Li, S. M. Lan, T. N. Yang, S. M. Lio, Thin Solid Films **516**, 99 (2007). "Fabrication of low-resistivity and gold-colored TiN films by halide chemical vapor deposition with a low [NH_3]/[$TiCl_4$] flow ratio"

[11] L. Zhou, W. Lanford, A. T. Ping, I. Adesida, J. W. Yang, A. Khan, Appl. Phys. Lett. **76**, 3451 (2000). "Issues concerning preparation of ohmic contacts to GaN"

[12] B. P. Luther, S. E. Mohney, T. N. Jackson, M. Asif Khan, Q. Chen and J. W. Yang, Appl. Phys. Lett. **70**, 57 (1997). "Investigation of the mechanism for ohmic contact formation in Al and Ti/Al contacts to n-type GaN"

[13] P. A. Hammond and D. R. S. Cumming, Microelectronics Engineering, **73**, 893 (2003). "Encapsulation of a liquid sensing microchip using SU-8 photoresist" [14] Toshiya Sakata, Masao Kamahori and Yuji Miyahara, Jpn. J. Appl. Phys. **44**, 2854 (2005). " DNA Analysis chip Based On Field-Effect Transistors"

[15] Jaewon Park, Hyun Soo Kim and Arum Han, **19**, 065016 (2009). "Micropatterning of Poly(dimethylsiloxane) using a photoresist lift-off technique for selective electrical insulation of microelectrode arrays"

[16] A. Gerardo Diaz-Quijada and Danial D. M. Wayner, Langmuir, **20**, 9607 (2004). "A simple Approach to Micropatterning and Surface Modification of Poly (dimethylsiloxane)"

[17] J. Garra, T. Long, J. Currie, T. Schneider, R. White and M. Paranjape, J. Vac. Sci. Technol. A, **20**, 975 (2002). "Dry etching of polydimethyl for microfluidic systems"

[18] Salil P. Desai, Brian M. Taff and Joel Voldman, Langmuir, **24**, 575 (2008). " A photopatternable Silicone for Biological Application"

CHAPTER 3

Immobilization And Detection Of OPH Enzymes

3.1 Enzymes

Enzymes are proteins that accelerate a biological reaction where the molecule at the beginning of the reaction or what is otherwise known as the substrate is converted into the product. Enzymes increase the rate of the reaction by decreasing the energy of activation and enzymes are specific about which reactions they catalyze. The specificity of enzymes has been explained by Fischer using "the lock and key model" which illustrates that the enzyme and the substrate have complementary geometrical shapes that fit exactly into one another[1].

3.2 Immobilization of Enzymes

Enzymes undergo physical and chemical changes during immobilization. These changes have to be taken into consideration during the enzyme immobilization process and the correct immobilization procedure has to be adopted. Immobilizing an enzyme leads to increased stability, ability for repeated use of the sensor surface and easy separation of the product and the enzyme. Enzyme immobilization can be achieved by applying different processes such as adsorption, covalent binding, entrapment, and encapsulation and cross-linking.

The following sections explain the different immobilization processes briefly.

3.2.1 Adsorption

Adsorption is a form of immobilization which is a non covalent form of interaction between the enzyme and the surface based on physical adsorption or ionic binding. The ionic binding can include hydrogen bonding, van der waals forces, hydrophobic interactions or salt linkages[2]. The unique feature of this method of immobilization maintains the enzyme activity and it costs less than the other immobilization methods but the process has a limitation that the binding is relatively weak as compared to covalent bonding[2].

3.2.2 Cross-Linking

Cross linking maintains the stability of enzymes without diluting the activity of the enzymes. One of the approaches is to crystallize the enzymes followed by cross-linking to either other enzyme molecules or to functional groups. The two most common cross-linking techniques are the avidin-biotin system and cross-linking using glutaraldehyde. This immobilization method increases the storage stability of enzymes[3].

3.2.3 Entrapment

The enzyme is blocked inside a polymeric network/gel which allows the substrate and the product to pass through but does not allow the enzyme to diffuse out of the polymeric gel. Some common polymeric networks that are used for entrapment are polyacrylamide, silicon rubber, polyvinyl alcohol or silical gel[4, 5]. One of the drawbacks of this method has been the leakage of smaller molecular weight enzymes.

3.2.4 Encapsulation

In encapsulation we can control the porosity of the enzyme. This method is very similar to

entrapment except that here the enzymes are captured in a semi-permeable membrane. Some of the common membranes are nylon, epoxy resins and butyl rubber[4].

3.2.5 Covalent binding

This form of binding is the most commonly used method for enzyme immobilization.

Even though this method is relatively difficult and costs more than the other methods it is preferred due to the robust binding that it offers and in addition there is no enzyme leakage.

In this method the surface is first activated by immobilizing a COOH terminating molecule and then exposed to an amine terminated enzyme in the presence of an activating agent so that they can form a covalent bond[6].

3.3 Organophosphates

Organophosphates (OP) are esters of phosphoric acid and the general structure is shown in figure 3.1. OP's contain an alkyl or an aryl side chain, O, S, F, C and or N and are covalently bonded to sulfur or oxygen. The phosphorous atom is bonded to four oxygen atoms in organophosphates. Some examples of organophosphate compounds are Sarin, Soman, Demeton-S, Paraxon and diisopropyl fluorophosphates which are all toxic cholinesterase inhibitors but they vary in their neurotoxicity[7, 8]. Paroxan, diisopropyl flurophosphate and Demeton-S are commercially available organophosphate pesticides. The phosphotriester bonds contain a P-O bond, phosphonothioates a P-S bond and the phosphonofluoridate a P-F bond.

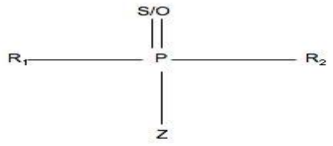

Figure 1: General structure of organophosphates

3.3.1 Toxicology of Organophosphates

Even though Organophosphates were first synthesized in the 1800's their toxic effects on the nervous system were only understood in 1932. This discovery led to them being used as pesticides and as chemical warfare agents. Organophosphates have since been used extensively in the agriculture industry. Annually around 60 million pounds of organophosphates are used for agriculture purposes. Organophosphates can be ingested, inhaled or even injected. Even though organophosphates are less toxic than chlorinated hydrocarbons they could still be carcinogenic[9]. OP pesticides inhibit the activity of acetylcholinesterase (AChE). The AChE enzyme is responsible for degrading the neurotransmitter acetylcholine (ACh) present in the central nervous system into choline and acetic acid.

Organophosphates inactivate AChE by phosphorylating the serine OH^- group present in the active site of AChE and this inactivation leads to the over stimulation of the nervous system. Some of the other serious effects of organophosphates include muscle paralysis and respiratory

problems. Long term exposure can lead to cancer and genetic problems. Due to these reasons the EPA has placed organophosphates among the first priority group to be reviewed under the food quality protection act. For example diazinon an OP insecticide normally used to control ants, cockroaches and fleas in residential buildings has been prohibited by the Environmental Protection Agency, since exposure to it was causing nervous system problems. In spite of the prohibition OP insecticide continues to be used until its stockpiles run out and is still legal to be used in certain cases [4, 10]. Analysis by the National Stream Quality Accounting Network and the U. S. Geological Survey discovered the presence of 11 Organophosphates in surface water. The concentration of OP was higher in the surface water as compared to ground water with Diazinon being the most common OP detected. Exposure to OP neurotoxins can negatively impact the nervous system after 21 days and there are no well defined treatment procedures available for this condition. As this is the case with the toxicity of OP's detection of OP's is extremely critical.

3.3.2 Organophosphate detection

The most widely used method for the detection of organophosphates is the enzyme based sensor. Some of the enzymes that have been used are acetylcholinesterase (AChE), butyrlcholinesterase, urease, and glucose oxidase, organophophorous acid anhydrolase (OPAA) and organophosphorous hydrolase (OPH). Out of these the cholinesterase based sensors are inhibition mode sensors. In the inhibition mode OP compounds binds irreversibly at the enzyme active site and hence decrease in sensor signal[11]. The limitation of using a cholinesterase based sensors are environmental factors which might reduce the cholinestrerase activity, lengthy incubation times and the inability to reuse them[11]. Cholinesterase based sensors also cannot distinguish between OP pesticides and OP chemical warfare agents.

These problems were overcome by using the catalytic receptor enzymes[11]. OPH and OPAA based enzymes are capable of selective recognition and hydrolysis of organophosphates. OPH is able to cleave P-O, P-F, P-S and P-CN bonds resulting in hydrolysis products which change the solution pH. Hydrolysis of phosphofluoridates results in a change in the pF as well as a change in the pH. OPAA is capable of cleaving P-F bonds but not P-O and P-S bonds[12]. Thus OPAA can be used to detect fluorine containing organophosphates.

This capability has been exploited to detect organophosphate pesticides and chemical warfare agents by using pHFET's[11].

3.4 Organophosphate hydrolase

Organophosphate hydrolase (OPH) is a metalloenzyme originally isolated from *pseudomonas dimunta* and has a dimeric crystal structure. OPH has been researched for the past 10 years[13, 14]. OPH cleaves P-O, P-F, P-S, P-CN bonds via an S_N2 type mechanism[11]. These are the bonds present in a different variety of OP containing compounds. The reaction between OPH and OP compounds results in a unique set of hydrolysis products which change the solution pH. This makes OPH ideal for detecting the OP containing compounds. The catalytic activity of OPH is determined by two divalent metal ions present in it such as Zn^{2+}, Cd^{2+}, Mn^{2+} or Ni^{2+}.

3.5 X-Ray photoelectron spectroscopy

In X-ray photoelectron spectroscopy (XPS) an incident x-ray photon ejects both core and valence electrons from the surface of a material. The kinetic energy of these ejected photoelectrons is measured, from which their atomic binding energy is calculated using Equation 1. From the binding energy value the bonding type and the concentration of surface species present on the material is calculated.

$$h\nu = B.E + K.E \text{---------- (1)}$$

Where,

$h\nu$= Incident photon energy

B.E= Atomic Binding energy of the photoelectrons

K.E= Kinetic energy of the photoelectrons

XPS can be used to detect all the elements except for hydrogen and helium. The depth that can be probed using the XPS is around 10nm and the lateral resolution from 5mm to 75μm.

An XPS spectrum consists of a relative intensity versus binding energy curve and the spectrum has a downward slope. In case of high atomic mass elements we get two peaks for the same element and this is due to the spin orbit coupling between the orbital magnetic field and the spin magnetic field of the electron. These spin orbit doublets are well separated easy to see, for example the Au 4f doublet is used to calibrate the XPS instrument.

The XPS instrument (Figure 3.2) consists of a UHV chamber where the sample holder is located, an X ray source and an electron spectrometer to calculate the photoelectron kinetic energy. Since the material is loosing electrons it becomes positively charged and thereby the electron binding energy is shifted to a higher value, hence precautions need to be taken by either grounding the sample or placing it in contact with a metallic substance in order to prevent it from getting charged during the X-ray bombardment. The binding energy of the elements can also shift due to their bonding with other atoms as bonding involves either the gain or loss of electrons. This bonding results in an increase with the orbital energies which can change the

binding energy value and a shift in the binding energy is commonly used to determine the bonding information present on the surface.

Figure 3.2: XPS system

3.5.1 Application of XPS in characterizing immobilized biomolecules

In the past 10 years there has been a rapid rise in using XPS to probe the bio-interface[15].

The advantage of XPS over other analytical techniques like surface Plasmon Resonance(SPR), Atomic Force Microscopy(AFM) and ellipsometry is that XPS can readily provide the chemical specific information in a relatively simple to interpret data format which other methods cannot. Attenuation of a specific element from the substrate can also be used to calculate the thickness of the biomolecular coatings[16]. XPS date is used to calculate the atomic percentage of elements present on the surface. This data is an indicator of the effectiveness of the biomolecular coatings. For example in the case of immobilized proteins the XPS signal exhibits peaks that correspond to carbon, oxygen, nitrogen and a few minor elements like sulphur and

oxygen. In some instances for a specific orientation or low surface immobilization density of the proteins might make sulphur or oxygen untraceable by XPS and in such cases the increase in the carbon to nitrogen ratio (C/N) is used to verify the immobilization chemistry[17].

In the case of DNA, XPS is used to characterize the immobilized DNA film by varying the immobilization time and the buffer strength of the immobilization buffer[18]. The principal elements that are monitored are carbon, nitrogen, oxygen and phosphorous. The presence of nitrogen and phosphorous are excellent indicators of adsorbed DNA since their presence is not affected by either sample preparation or handling. The relatively low percentage of phosphorous in DNA as compared to other principal elements might make it untraceable by XPS and the higher XPS cross section of nitrogen makes it the preferred element to verify the immobilization chemistry[19]. High resolution scans of C1s, N1s, P2p and S2p peak are plotted to obtain detailed information of the binding. The predicted stoichometry of the DNA molecule is Phosphorous/Nitrogen= 0.3, Oxygen/Nitrogen= 1.7 and Carbon/Nitrogen= 2.8[18]. Since it is easier for the sample to get contaminated by carbon during handling, the Phosphorous/Nitrogen and Oxygen/Nitrogen ratios are commonly taken into consideration to conclude about the immobilized DNA. In the case of thiolated DNA immobilized on gold the S2p peak is around 162ev[20]. For DNA immobilized on gold which the most preferred immobilizing metal, the attenuation of the gold signal is used to calculate the DNA surface density.

3.6 Immobilization of OPH

3.6.1 Materials

11-Mercaptoundecanoic acid (MUA), 3-Mercaptopropionic acid (MPA), Paraxon (diethyl-p-nitrophenyl phosphate), 1-ethyl-3-(3-dimethylaminopropyl) carbodiimide (EDC) and N-hydroxysuccinimide (NHS) were purchased from Sigma- Aldrich. Organophosphorous hydrolase (OPH) is obtained from J. Wild (Texas A&M University). All other chemicals and reagents were of analytical grade and are obtained from Sigma- Aldrich (St. Louis, MO).

Water used is from Millipore Direct-Q water system and has a resistivity of 18 $M\Omega\ cm^{-2}$.

3.6.2 Preparation of slides for Immobilization

To remove any organic impurities the glass slides are rinsed in piranha solution (30% H_2O_2 and 70% concentration H_2SO_4) for two minutes followed by acetone, methanol and DI water for five minutes each in an ultrasonicator. The cleaned glass slides are than blown dry using N_2 gas. An adhesion layer of Chromium (10nm) followed by Au (200nm) is sputtered on the glass slides using a DC magnetron sputtering system. The Gold coated glass slides are rinsed in piranha solution for two minutes followed by DI water and then plasma cleaned for two minutes. This results in a clean and a hydrophilized surface.

3.6.3 Immobilization

After the plasma cleaning the gold coated glass slides are immediately dipped in a 1 mM solution of 11-mercaptoundeconoic acid (MUA) solution (dissolved in ethanol) for 12 hours. After this the samples are thoroughly rinsed in ethanol and dried with nitrogen gas. MUA forms

a self assembled monolayer (SAM) on gold (Figure 3.3) by a two step process. In the first step the thiol group gets deprotonized (equation 2) and forms a noncovalent bond with gold.

In the second step the interaction between the –COOH- groups and also the methylene groups of the hydrocarbon chains result in a 30^0 orientation of the SAM with respect to the gold surface and the parallel arrangement of the SAM[1, 2] with respect to each other.

$$RSH + Au\text{----------}RS\text{-}Au + e^- + H^+ \text{ ---------- (2)}$$

This immobilization chemistry is verified by X- ray photoelectron spectrometry (XPS). Mg-Kα was used as the X-ray source. The vacuum pressure during the measurement was lower than $5x10^{-8}$ torr. Binding energy of the photoelectrons was calibrated using Au. Curve fitting of the photoemission spectra was done after a Shirley type background subtraction.

As seen in figure 4 the XPS plot shows the presence of Carbon, Oxygen, sulphur and gold. The presence of sulphur in the XPS plot is from the thiol group of MUA. This plot is used as a reference and compared to the XPS plots after the OPH immobilization to standardize the immobilization conditions. The atomic percentage of the surface elements are also calculated as shown in Table 3.1 .

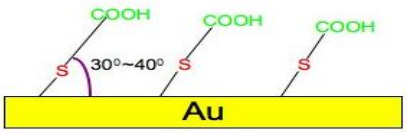

Figure 3: Immobilization of MUA on gold

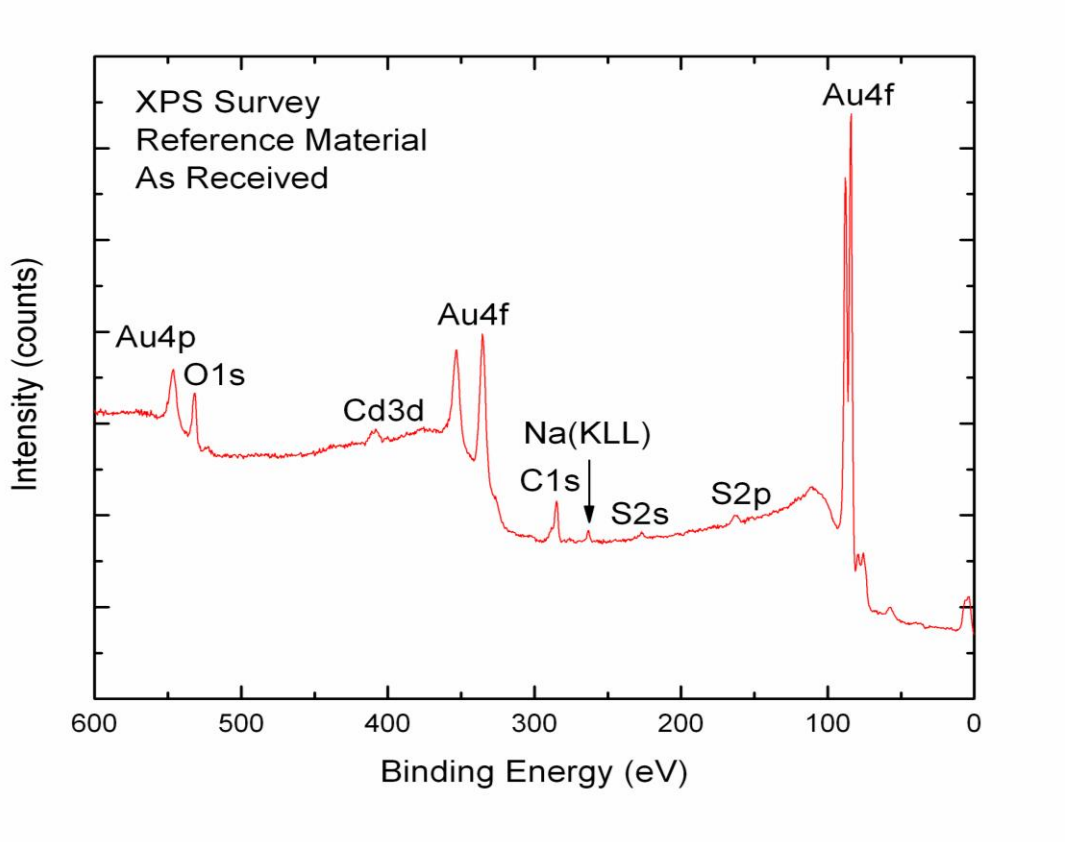

Figure 3.4: XPS spectrum of MUA immobilized on gold

Element	Oxygen	Carbon	Sulphur	Gold	Cadmium
Atomic percentage (%)	17	45	8	29	0.6

Table 3.1: Atomic percentage of MUA elements immobilized on gold

3.6.4 Immobilization of OPH

After the immobilization of MUA the surface is cleaned with ethanol and it is then exposed to 1mM of 1- Ethyl-3-[3-dimethylaminopropyl] carbodiimide hydrochloride (EDC) and 5mM of N-hydroxysucciniimide (NHS) for two hours. The EDC and the NHS mixture are prepared in cold DI water at 4^0C since their activity is high in cold water. The surface is then washed with DI water and then exposed to OPH for 12 hours at 4^0C. EDC in the presence of NHS helps in converting the carboxyl groups to amine reactive esters which aid in the bond formation with the amine group of OPH (Figure 3.5). XPS of the gold substrate confirms the OPH immobilization (Figure 3.6). The presence of sodium and chlorine is from the Phosphate buffered saline (PBS). The atomic percentage of sulphur and gold is found to decrease after the OPH immobilization which is expected since the immobilized OPH attenuates the signal from these elements. Curve fitting analysis of the C1s spectrum (Figure 3.7) results in two peaks for the carbon atom. One peak is at 285.06 eV corresponding to the C-C and C-H bonds[21]and the other peak is at 288.29 eV corresponding to the C=O-N bonding[21, 22]. The N1s spectra (Figure 3.8) with a peak centered at 400.9ev arises from nitrogen atom in amines and amides[23]. These peaks confirm the immobilization of OPH.

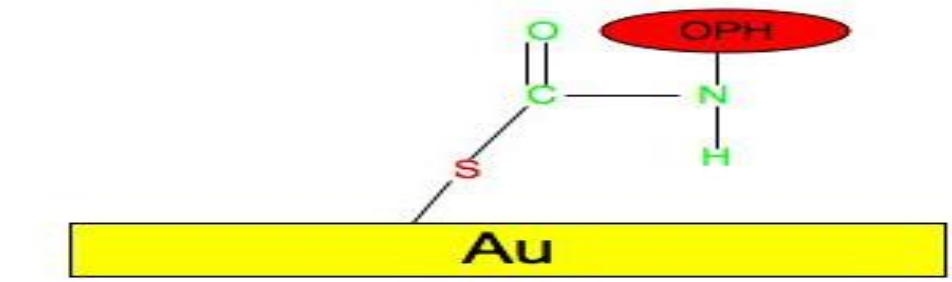

Figure 5: Immobilization of OPH

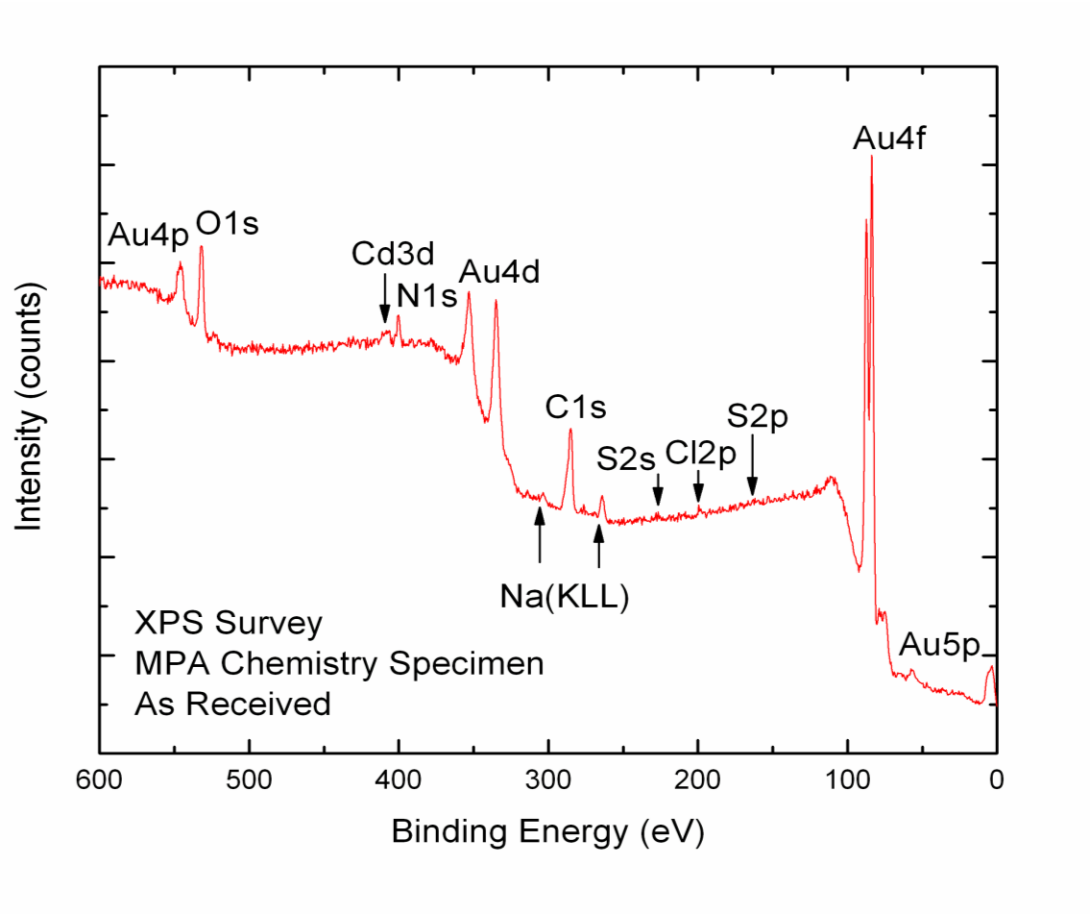

Figure 3.6: XPS spectrum of OPH immobilized on gold

Elements	Nitrogen	Oxygen	Carbon	Gold	Sulphur	Cadmium
Atomic Percentage(%)	9	15	61	16	<1	<1

Table 3.2: Atomic percentage of OPH immobilized on gold

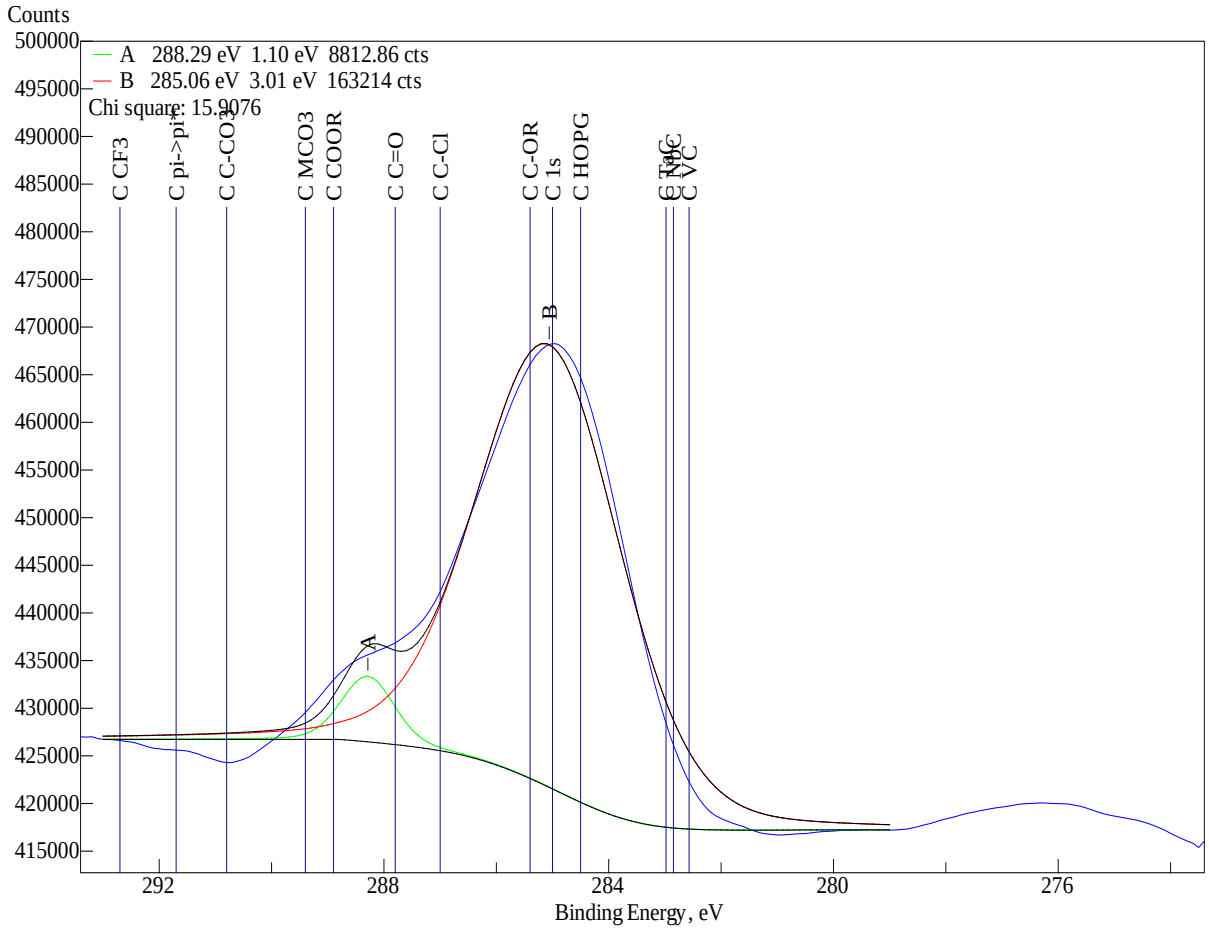

Figure 3.7: High resolution scan of C1s

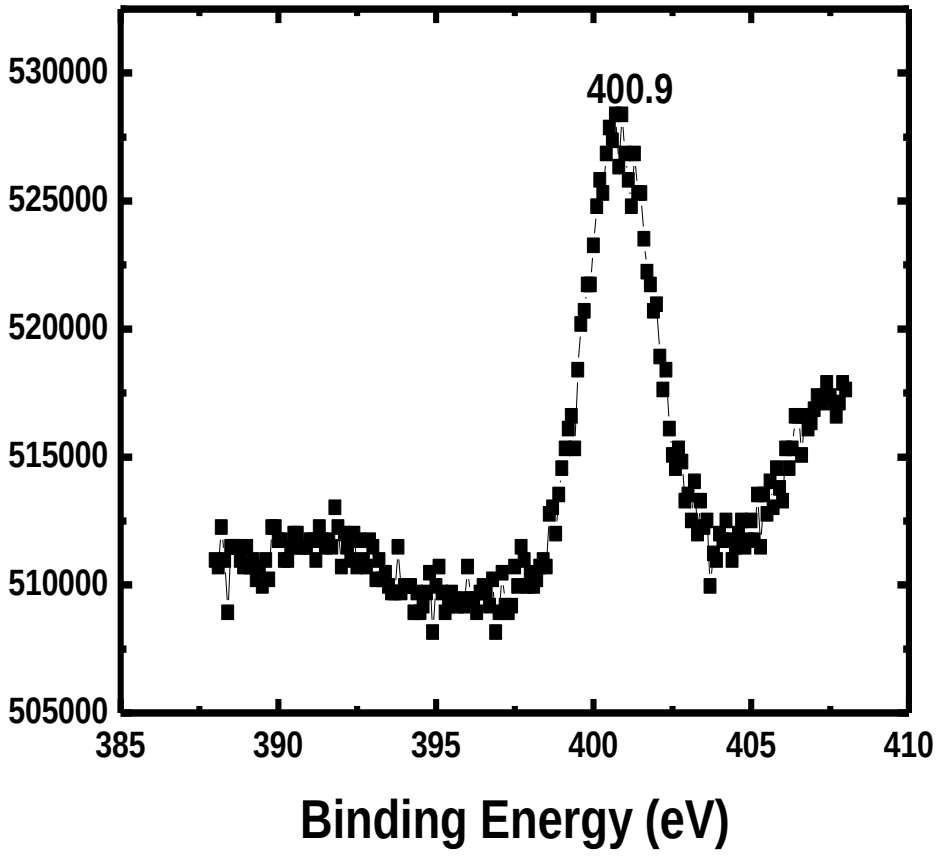

Figure 3.8: High resolution scan of N1s with a peak centered at 400.9ev

3.7 Detection of OPH using AlGaN/GaN HEMT

Since the hydrolysis of organophosphates (OP) by the catalytic receptor enzyme organophosphates hydrolase (OPH) results in a change in the solution pH, a pHFET can be used to detect OP. Using a catalytic receptor enzyme like OPH overcomes the problems associated

with inhibition mode biosensors like non-reusability and false positives due to environmental factors.

The OPH enzyme can be directly immobilized on the gate surface and can then be exposed to OP compounds. The pHFET needs to be highly sensitive and stable which requires that the sensing material be chemically stable. GaN and its alloy AlGaN have no know chemical etchants which makes them chemically very stable. The formation of a high mobility and high density 2 dimensional electron gas (2DEG) channel provides a high sensitivity. Since the pHFET will be operated in a liquid environment the encapsulation needs to be stable and have good adhesivity with the sensor material to prevent any electrical short-circuits. Photodefinable PDMS (WL-5150) from Dow Corning is used for this encapsulation purpose (Figure 3.10). The entire device area except the gate surface is encapsulated with a 20μm thick layer.

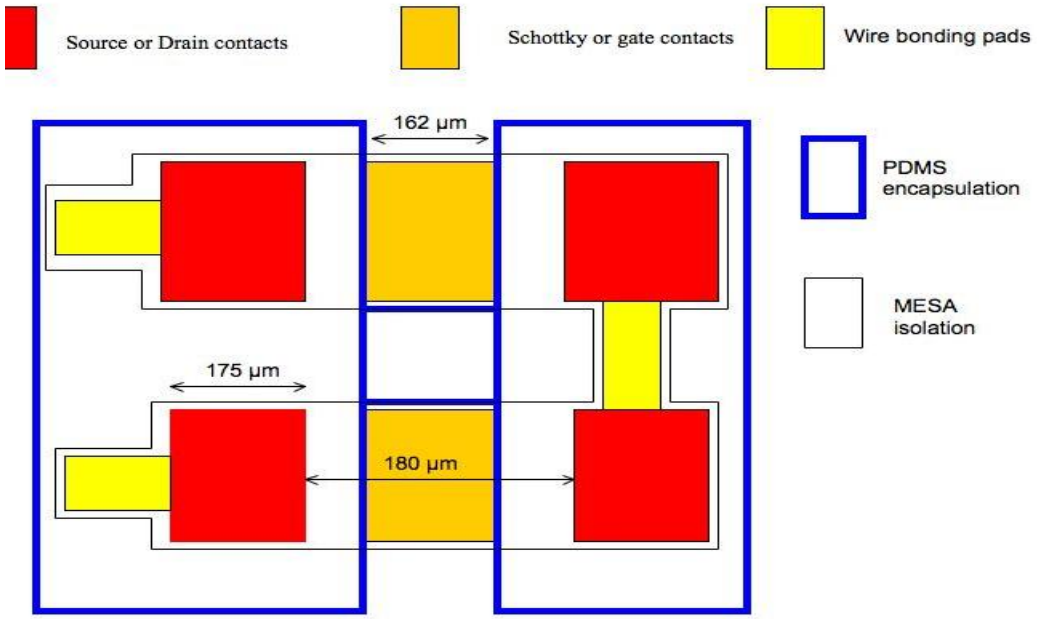

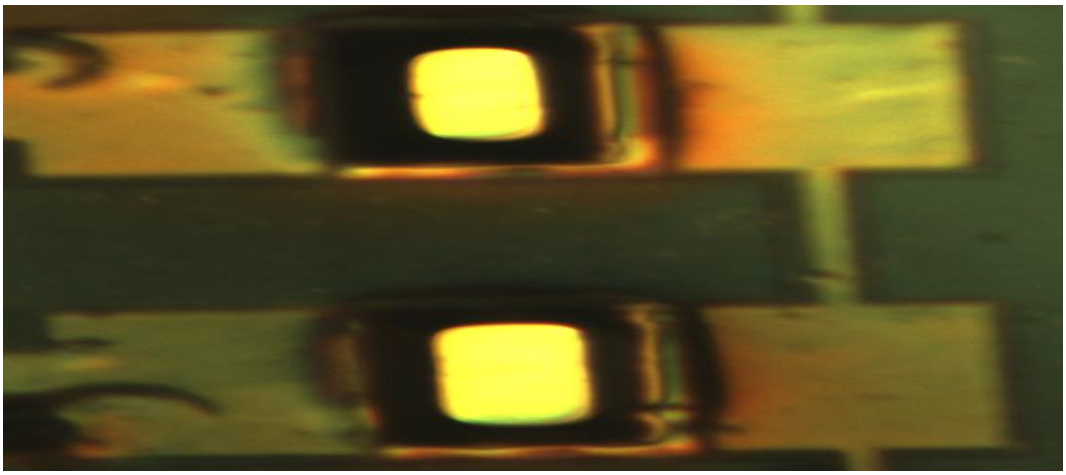

Figure 3.10: Picture of the PDMS encapsulated device

Unlike amperometric-based sensors, AlGaN/GaN HEMT sensors do not require a fixed reference electrode in the solution to measure the potential applied, since the sensing with the HEMT sensor was measured through the change in the drain current of the HEMT with a change in the surface charges[23]. This simplifies the experimental setup and also reduces the volume of the reagents to be used.

The OPH enzyme was immobilized on the gate surface of the HEMT using the immobilization chemistry described previously in section 3.6.4. The immobilization is carried out by pippeting 50~60µl of the immobilization solution on the device. The device which is attached to a gold patterned ceramic substrate for the purpose of wire bonding is then kept in a Petri dish which is maintained at high humidity to prevent any evaporation of the immobilization buffer (Figure 3.11).

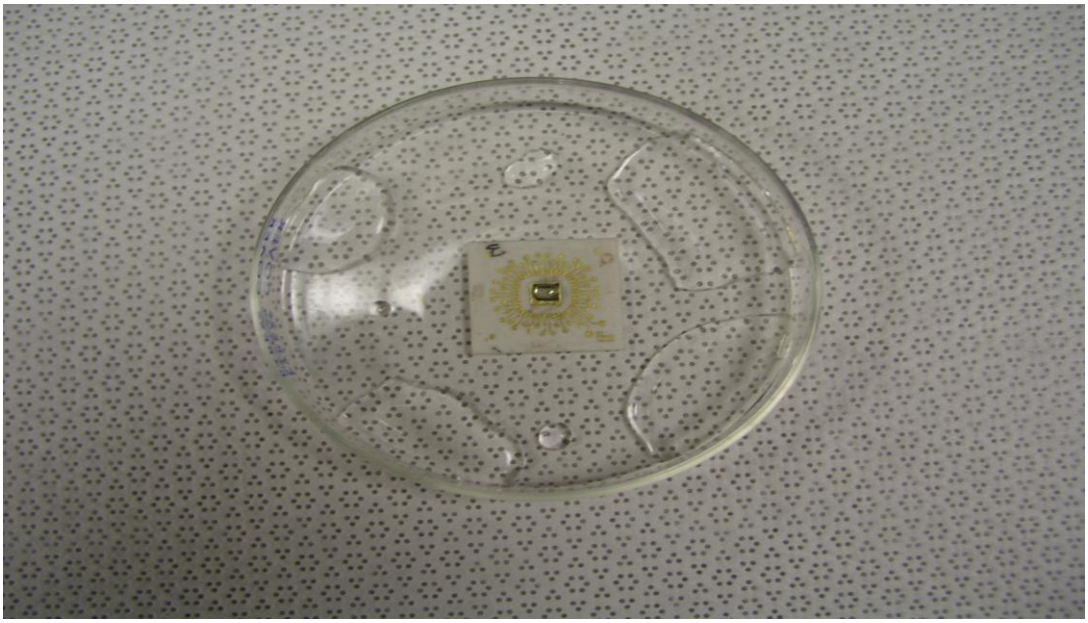

Figure 3.11: Immobilization of OPH on the sensor surface

The I_{ds}- V_{ds} characteristics of the device at zero gate bias are measured after the cleaning and before any immobilization steps were carried out (Figure 3.12).

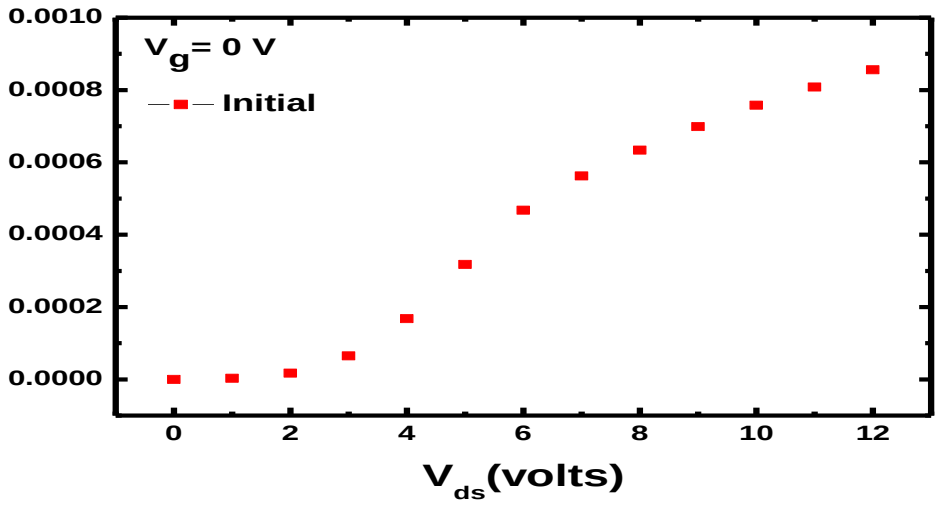

Figure 3.12: Initial I_{ds}- V_{ds} characteristics of the device

The I_{ds}- V_{ds} characteristics are measured before and after each immobilization step. As shown in figure 3.13 the drain current of the HEMT decreased by 453 μA after the MUA immobilization due to the negative charge of the thiols[24]. There was no appreciable change in the current after the EDC-NHS activation as shown in Figure 14. After the OPH immobilization the drain current of the HEMT increases by 119 μA (Figure 3.15) due to the positive charge of the amines[24].

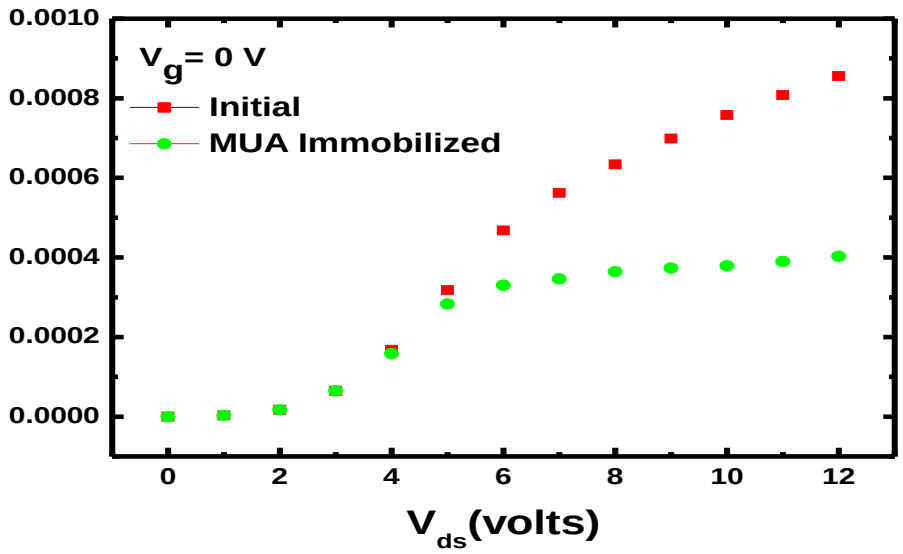

Figure 3.13: I_{ds}- V_{ds} characteristics of the device before and after MUA immobilization

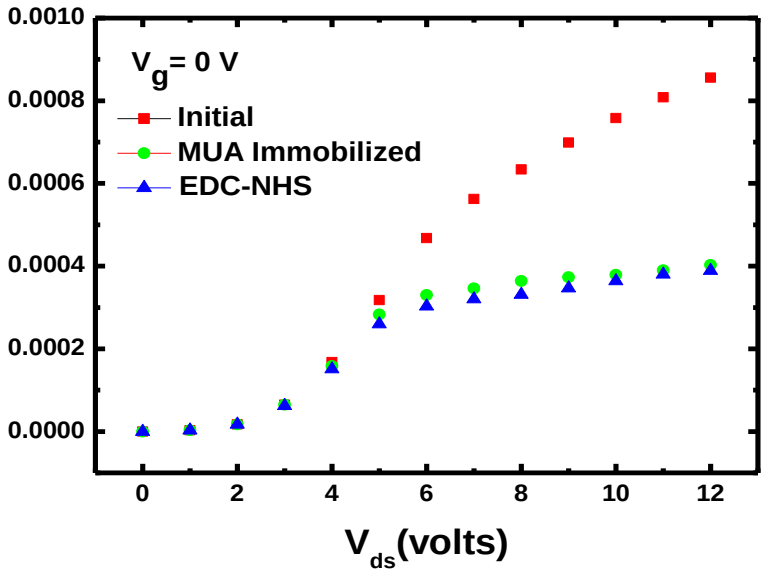

Figure 3.14: I_{ds}- V_{ds} characteristics of the device after EDC–NHS activation

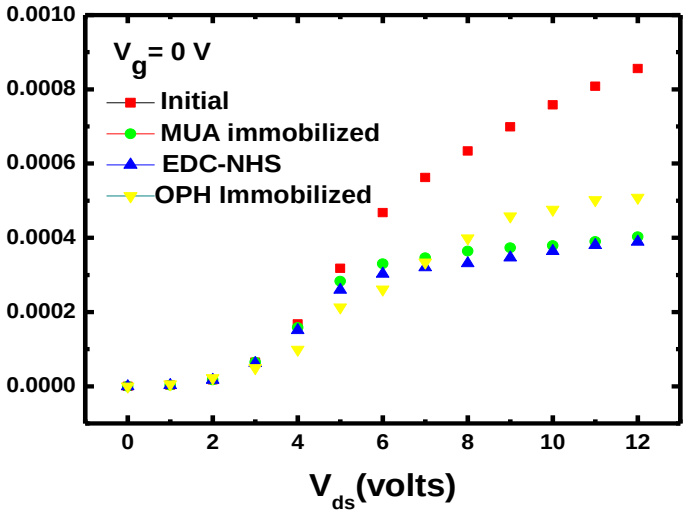

Figure 3.15: I_{ds}- V_{ds} characteristics of the device after OPH immobilization

3.8 Conclusion

The key conclusions from this study are that it is possible to immobilize OPH enzyme on the gold surface of an AlGaN/GaN HEMT for the purpose of detection of OP neurotoxins. Subsequently the immobilization can be monitored real time by measuring the I_{ds}- V_{ds} characteristics of the pHFET. More importantly this biosensor can also be used for continuous remote monitoring and analysis.

3.9 References

[1] David L. Nelson, Michael M. Cox, Principles of Biochemistry, New York, W. H. Freeman and Company, 2005.

[2] Jose M. Guisan, Immobilization of Enzymes and cells, New Jersey, Humana Press Inc. 2006.

[3] C. P. Govardhan, Curr Opin Biotechnol. **10**, 331 (1999). "Crosslinking of enzymes for improved stability and performance"

[4] Sheetal palliwal dissertations

[5] P. W. Carr and L. D. Bowers, Immobilized Enzymes in Analytica and Clinical Chemistry: Fundamentals and Applications, John Wiley & Sons, New York, 1980.

[6] http://www.piercenet.com/products/browse.cfm?fldID=02030312

[7] A. L. Simonian, A. W. Flounders, J. R. Wild, Electroanalysis, **16**, 1896 (2004). "FET-Based Biosensors for the Direct Detection of Organophosphate Neurotoxins"

[8] D. P. Dumas, H. D. Durst, W. G. Landis, F. M. Raushel, J. R. Wild, Arch. Biochem. Biophys. **277**, 155 (1989). "Inactivation of Organophosphorus Nerve Agents by the Phosphotriesterase from *Pseudomonas diminuta"*

[9] G. A. H. C. Chemical Terms, Available From http://frontierassoc.net/greenaffordablehousing/tools/ChemicalTerms.shtml.

[10] Insecticides, Available from: http://users.ren.com/jkimball.ma.ultranet/biologypages/I/Insecticides.html

[11] A. L. Simonian, A. W. Flounders, J. R. Wild, Electroanalysis, **16**, 1896 (2004). "FET-Based Biosensors for The Direct Detection of Organophosphate neurotoxins"

[12] A. L. Simonian, J. K. Grimsley, A. W. Flounders, J. S. Scchoeniger, Tu-Chen Cheng, J. J. Defrank, J. R. Wild, Anal. Chim. Acta, **442**, 15 (2001). "Enzyme –based biosensor for the direct detection of fluorine –containing organophosphates"

[13] C. S. McDaniel, L. L. Harper, J. R. Wild, J. Bacteriol. **170**, 2306 (1998). "Cloning and Sequencing of a Plasmid-Borne Gene (OPD) Encoding a Phopshotriesterase"

[14] D. P. Dumas, J. R. Wild, F. M. Raushel, Biotech. Appl. Biochem. **11**, 235 (1989). "Purification and properties of the phosphotriesterase from Pseudomonas diminuta"

[14] K. Lai, N. J. Stolowich, J. R. Wild, Arch. Biochem. Biophys. **318**, 59 (1995). "

[15] D. G. Castner, B. D. Ratner, Surf. Sci. **500**, 28 (2002). "Biomedical surface science: Foundations to frontiers"

[16] S. L. Mcarthur, K. M. McLean, S. T. John Haw, H. J. Griesser, Biomaterials, **22**, 3295 (2001). "XPS and surface-MALDI-MS characteristics of worn HEMA-based contact lenses"

[17] S. L. McArthur, Surf. Interface Anal. **38**, 1380 (2006). "Applications of XPS in bioengineering"

[18] C. Y. Lee, P. Gong, G. M. Harbers, D. W. Grainger, D. G. Castner, L. J. Gamble, Anal. Chem. **78**, 3316 (2006). "Surface Coverage and Structure of Mixed DNA/Alkylthiol Monolayers on Gold: Characterization by XPS, NEXAFS, and Fluorescence Intensity Measurements"

[19] A. Lapiciki, F. Sakamoto, A. Sandhu, Jpn. J. Appl. Phys. **46**, L49 (2007). "Monitoring DNA Hybridization by Quantification of Nitrogen Content Using X-Ray Photoelectron Spectroscopy"

[20] http://srdata.nist.gov/xps/.

[21] E. Briand, M. Salmain, C. Compere, C. M. Pradier. Biosens. Bioelectron. **15**, 615 (2000). "Immobilization of Protein A on SAMs for the elaboration of immunosensors"

[22] M. Wirde, U. Gelius, L. Nyholm, Langmuir, **15**, 6370 (1999). "Self- Assembled Monolayers of Cystamine Cysteamine on Gold Studied by XPS and Voltammetry"

[23] B. H. Chu, Y. L. Wang, B. S. Kang, F. Ren, C. Y. Chang, Y. L. Wang, S. J. Pearton, A. V. Glushakov, D. M. Dennis, J. W. Johnson, P. Rajagopal, J. C. Roberts, E. L. Piner, and K. J. Linthicum, Appl. Phys. Lett. **93**, 042114 (2008). "Enzyme-based lactic acid detection using AlGaN/GaN high electron mobility transistors with ZnO nanorods grown on the gate region"

[24] D. S. Kim, J. E. Park, J. K. Shin, P. K. Kim, G. Lim and S. Shoji, Sens. Actuators B ,**117**, 488 (2007). "An extended gate FET-based biosensor integrated with a Si microfluidic channel for detection of protein complexes"

CHAPTER 4

DNA Detection Using AlGaN/GaN High Electron Mobility Transistor

4.1 Introduction

Detection of deoxyribonucleic acid (DNA) in a fast, sensitive and reliable manner is necessary in areas of food safety and medical research. Since a DNA carries the genetic information and this genetic information can be passed to other cells and change their genotypes, it is possible that a harmful bacterial cell which is not active can transform its information through the DNA to other active and non-virulent cells resulting in a virulent cell. This makes detecting pathogenic DNA paramount in food safety. In areas of medical research the present methods of gene sequencing are slow, laborious and expensive. The problems of longer detection time, higher cost and the inability to perform the detection in remote locations associated with the present DNA detection mechanism can be overcome by utilizing the concept of DNA hybridization. DNA hybridization occurs in 15-20 minutes and when combined with a field effect transistor (FET) which can convert a charge effect into an electrical signal can lead to a fast, sensitive and miniature sensor.

In order for a FET to function as a DNA hybridization sensor it is important to immobilize the probe ssDNA on the sensor surface. This immobilization must be robust in order to enable reusability and should cover the sensor surface to the required density of 10^{12} to 10^{13} probes/cm^2 to make the FET sensitive enough to detect the DNA hybridization event[1, 2].

4.2 Immobilization of DNA

The different types of immobilization mechanisms are physisorption, covalent attachment, affinity reactions and ionic binding. The immobilization method utilized is selected based on the choice of the substrate and the sensing mechanism desired.

4.2.1 Immobilization using affinity reactions between avidin and biotin

In this method the high affinity ($K_d=10^{-15}$) of avidin and streptavidin towards biotin is exploited. The DNA is attached to the biotin molecule with the help of a spacer. This biofunctionalized biotin molecule is then coupled to either avidin or streptavidin. Avidin exhibits a strong binding towards biotin at a pH of 4.

Avidin is a glycoprotein extracted from chicken egg white. Streptavidin on the other hand is prepared from the recombinant bacterial strain *Streptomyces avidinii*.

The use of streptavidin has found to give a higher signal to noise ratio as compared to avidin. Streptavidin has lower solubility in water than avidin resulting in less non-specific binding. The coupling between biotin and strepatvidin/biotin is extremely strong and can only be denatured in extreme conditions like a pH of 10 or higher[3].

4.2.2 Immobilization by ionic binding

In ionic binding the electrostatic interaction between the negatively charged phosphate group of the nucleic acids and the positively charged amine groups is utilized. The Self Assembled Monolayer (SAM) on the surface is modified so that the amine group is protonated. In case of a carboxylic acid terminated SAM, the biomolecule is coupled via Poly-L- Lysine[3].

4.2.3 Immobilization using covalent binding

The oligonucleotide is chemically modified either at the 5' end or at the 3'end. This chemically modified nucleotide can then be covalently bonded to a Self Assembled Monolayer (SAM). In amine modified DNA can be coupled to a SAM with a carboxylic acid terminal group by exposure to 1-Ethyl-3-[3-dimethylaminopropyl]carbodiimide hydrochloride (EDC) and *N*-hydroxysulfosuccinimide (NHS). This reaction has to carry out in a pH range of 7-9. This kind of coupling results in larger distance and more flexibility between the biomolecule and the surface[3, 4].Covalent attachment (Table 1) is predominantly used in biochips since it offers a possibility of reusability.

Anchor group	Binding partner	Reaction
-COOH	$-NH_2$	carbodiimide
$-NH_2$	$-NH_2$	Glutaraldehyde
-OH	$-NH_2$	bromcyane

Table 4-1: Some methods of covalent coupling to biomolecules

4.2.4 Formation of Mixed Self Assembled Monolayer

Mixed Self Assembled Monolayers (SAM) are used to reduce the problem of steric hindrance otherwise present between adjacent monolayers. The most commonly applied method to pattern mixed self assembled monolayers is to first immobilize the thiolated DNA and then

expose the surface to mercaptohexanol (MCH)[5] or to use a combination of thiolated DNA along with 6-hydroxy-1-hexanol (6-HHT)[6]. The DNA strands can get adsorbed onto the substrate by the nucleic acids rather than the bonding that is preferred. This increases the probability of non-specific binding since not all the nucleic acids are available for hybridization. MCH or 6-HHT desorb the DNA strands adsorbed on the substrate by their nucleic acids and covalently bond to those sites. This reduces the probability of non-specific binding and hence increases the hybridization efficiency and the sensitivity of the sensor.

4.2.5 Efficiency of hybridization

The factors that affect the hybridization efficiency are DNA probe length, surface coverage density of the ssDNA and the length of the linker molecule between the oligonucleotides and the surface. Among these the length of the linker molecule is the most important in determining the hybridization efficiency. For example 100% hybridization efficiency was achieved on gold by using a six methylene linker molecule. The optimal surface coverage density for the most efficient hybridization density has been determined to be in the range of 10^{12} to 10^{13} probes/cm^{-2}. Experimentally it has been determined that the optimum DNA probe length for maximum hybridization efficiency is 24 bases[3, 7]. DNA probes longer than 24 bases have a tendency to form random coil configurations and hence reduce the hybridization efficiency.

4.3 Experimental

4.3.1 Materials

Pottasium phosphate monobasic and 6-mercapto-1-hexanol (MCH) were obtained from Sigma Aldrich (St. Louis, MO). Tween 20, EDTA, Sodium phosphate and Sodium chloride was obtained from Fisher Scientific (Hampton, NH). Reductacryl reagent was obtained from CALBIOCHEM. All water used in the preparation and rinsing of the buffer solutions was Type I water prepared in a milliporre system and determined to be $\leq$ 18.2 mΩ.

4.3.2 Immobilization of DNA

To remove any organic impurities the 5mmX 5mm glass slides are rinsed in piranha solution (30% H_2O_2 and 70% concentration H_2SO_4) for two minutes followed by acetone, methanol and DI water for five minutes each in an ultrasonicator. The glass slides are than blown dry using N_2 gas. An adhesion layer of Chromium (10nm) followed by gold (200nm) is sputtered on the glass slides using a DC magnetron sputtering system. The Gold coated glass slides are rinsed in piranha solution for two minutes followed by DI water and are then plasma cleaned for two minutes. This results in a clean and a hydrophilized surface.

To standardize the immobilization protocol three gold coated glass slides are exposed to 60 µl of thiolated DNA (1µM) in 0.1 M phosphate buffer of pH 7 for a period of 2, 4 and 6 hours respectively. XPS data obtained from these samples is then used to calculate the atomic percentage of the elements present on the surface. This data is then compared to the data from a "reference gold slide" not exposed to the thiolated DNA. These spectra are used to optimize the immobilization conditions. Auger Electron Spectroscopy (AES) analysis is conducted on these

samples since it has a higher elemental sensitivity to sulphur as compared to XPS for the beam energy used.

Element	Gold	Carbon	Oxygen	Sulphur
Atomic percentage (%)	74	26	0	0

Table 4.2: Atomic percentage of elements in the reference gold slide

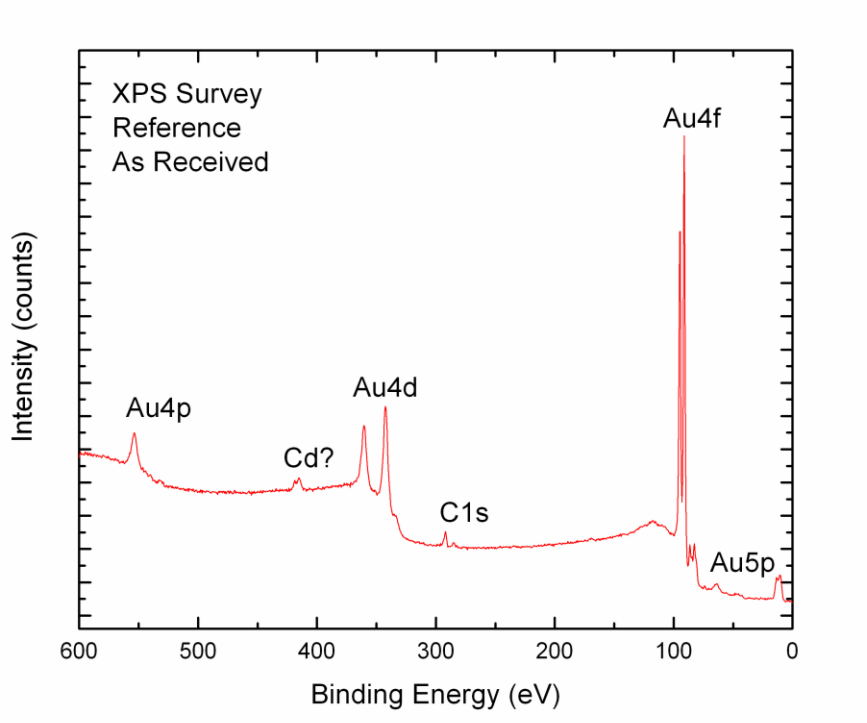

Figure 4.1: XPS spectra of reference gold slide

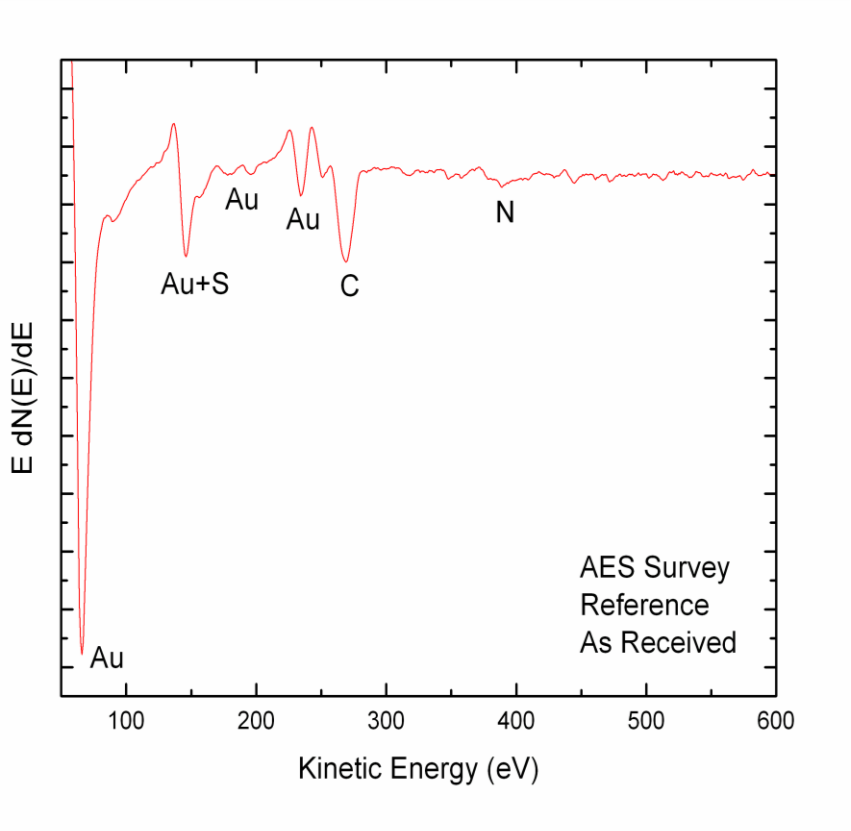

Figure 4.2: AES spectra of reference gold slide

As seen in figure 1 the XPS spectra of the reference gold slide indicates the absence of sulphur. Gold and Carbon are the only elements detected. The AES spectra (Figure 2) indicates the presence of trace amounts of sulphur (<1%). This contamination is possible during sputtering.

Element	Gold	Carbon	Oxygen	Sulphur
Atomic concentration(%)	27	65	7	2

Table 4.3: Atomic percentage of elements in the gold slide exposed to the thiolated DNA for 12 hours

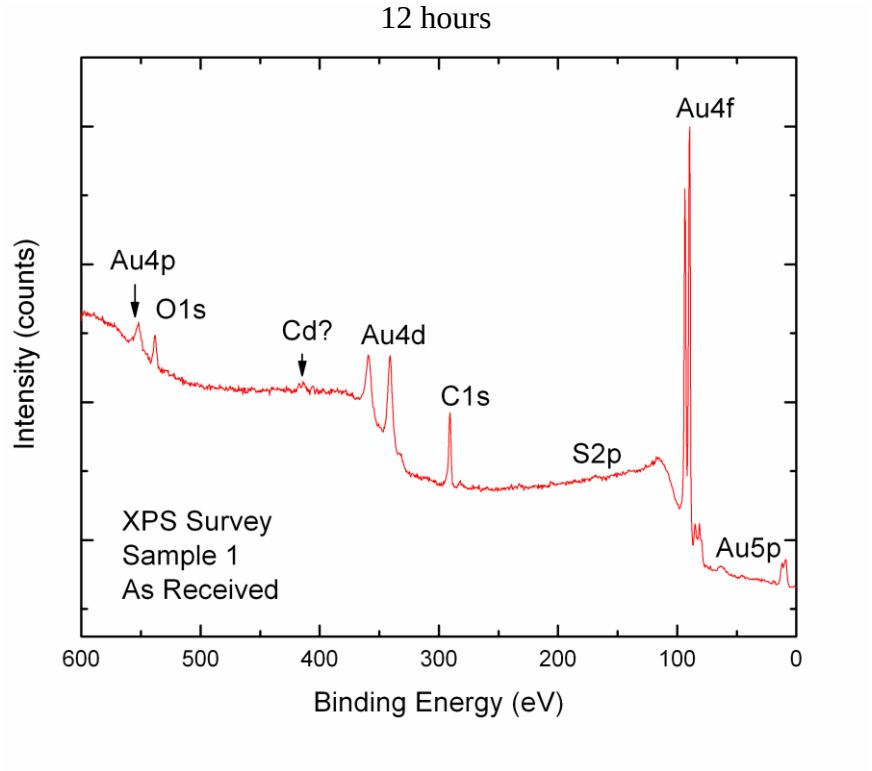

Figure 4.4: XPS survey of the gold slide exposed to thiolated DNA for 12 hours

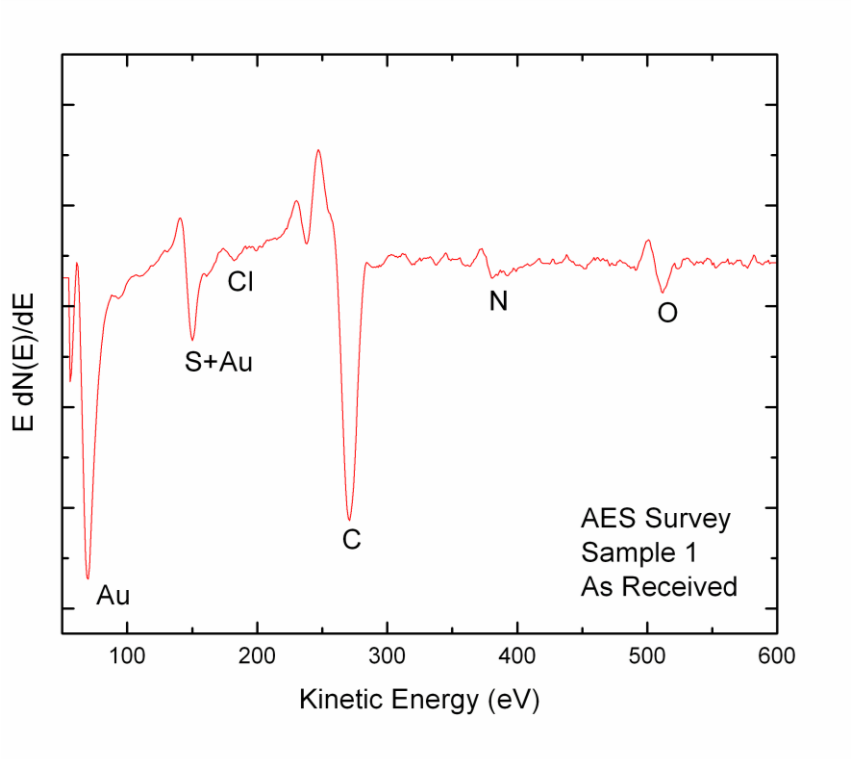

Figure 4.5: AES survey of the gold slide exposed to thiolated DNA for 12 hours

XPS survey of the gold slides exposed to the thiolated DNA indicates 2, 5 and 4% of sulphur present in the slides exposed for 12, 6 and 2 hours respectively. The higher percentage of sulphur indicated a higher immobilization density of the thiolated ssDNA. The atomic percentage of oxygen detected and the attenuation of the gold signal as comapared to the reference gold slide is a maximum in the slide exposed to the thiolated DNA for 6 hours. Hence this concludes that the optimum immobilization time for the formation of uniform monolayers of thiolated DNA on the gold is 6 hours[8-11].

Element	Gold	Carbon	Oxygen	Sulphur
Atomic concentration(%)	24	58	13	5

Table 4.4: Atomic percentage of elements in the gold slide exposed to the thiolated DNA for 6 hours

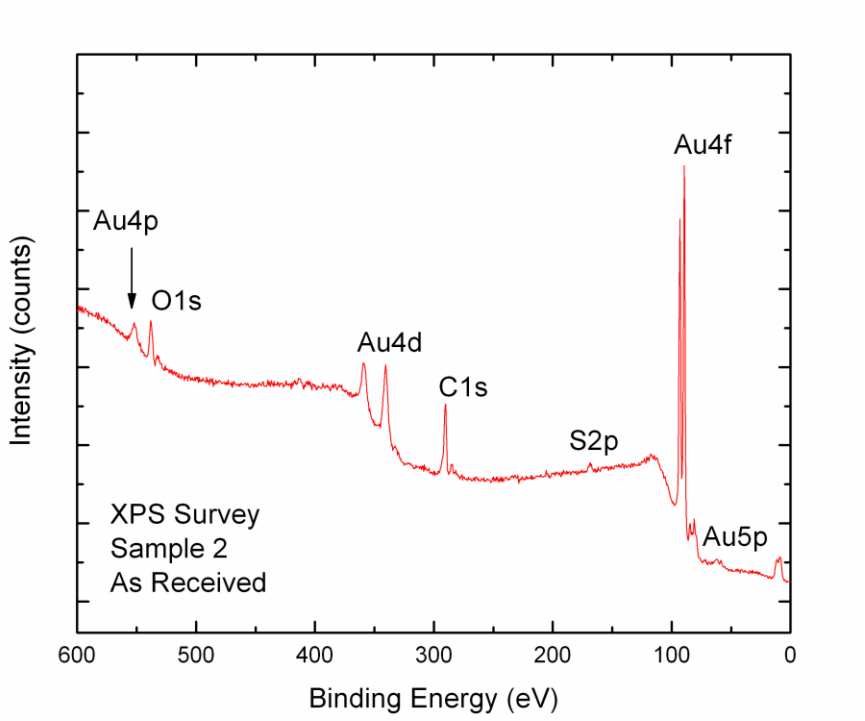

Figure 4.5: XPS survey of the gold slide exposed to thiolated DNA for 6 hours

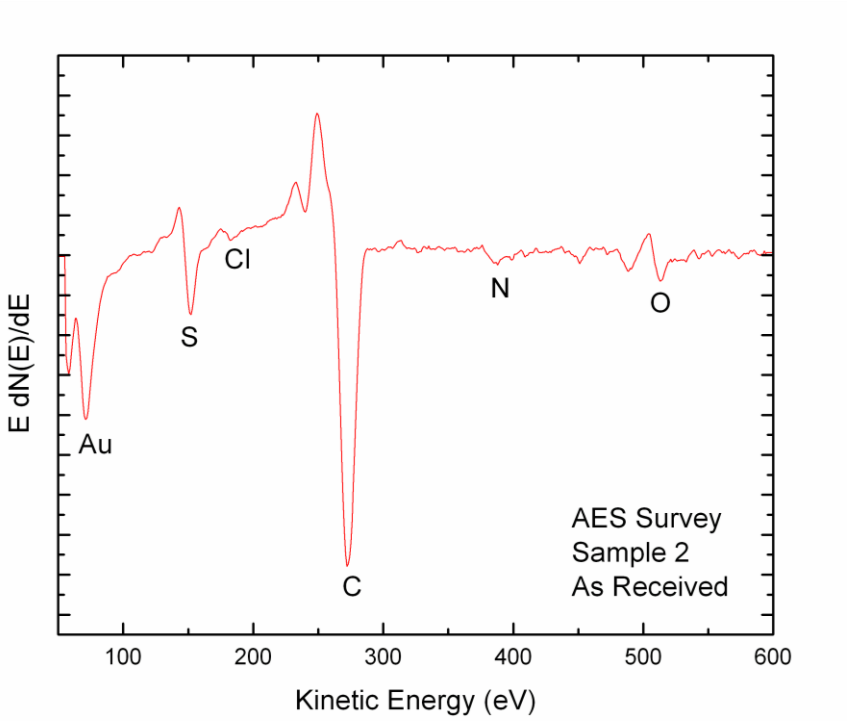

Figure 4.6: AES survey of the gold slide exposed to thiolated DNA for 6 hours

Element	Gold	Carbon	Oxygen	Sulphur
Atomic concentration(%)	40	45	11	4

Table 4.5: Atomic percentage of elements in the gold slide exposed to thiolated DNA for 2 hours

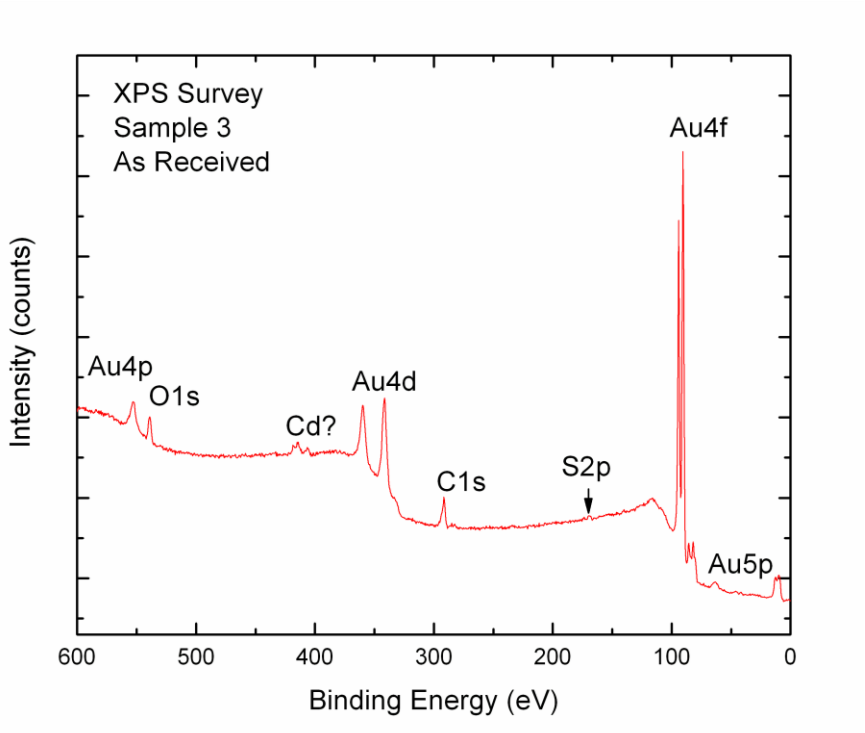

Figure 4.7: XPS survey of the gold slide exposed to thiolated DNA for 2 hours

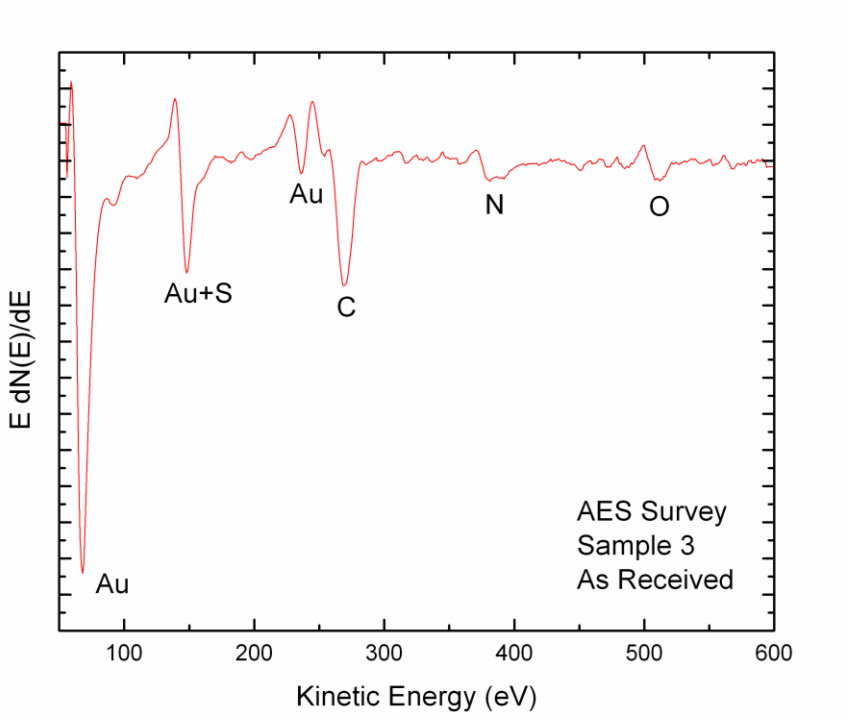

Figure 4.8: AES survey of the gold slide exposed to thiolated DNA for 2 hours

The high resolution scan of the S2p peak for the biofunctionalized gold slide shows a wide peak with a peak binding energy of 162.7eV. This binding energy indicates sulphur gold binding[9-11]. The wide S2p peak shows multiplicity of bonding states like S-H, S-C and S-P.

4.4 DNA detection

The AlGaN/GaN HEMT device was encapsulated with a 20µm thick PDMS layer except for the gate contact of the device.

In order to immobilize the probe DNA on the gold sputtered gate surface 60µl of the immobilization buffer containing 4µM of the 3'- thiolated DNA in 0.1 M phosphate buffer, pH 7 for 6 hours. The I_d-V_{ds} characteristics of the device at zero gate bias were measured during this immobilization process (Figure 9). The drain current of the HEMT decreases by 2056 µA due to negative charge of the immobilized DNA[12]. After a period of 6 hours the drain current remains stable. This confirms that a stable SAM of the thiolated DNA has formed on the sensor surface.

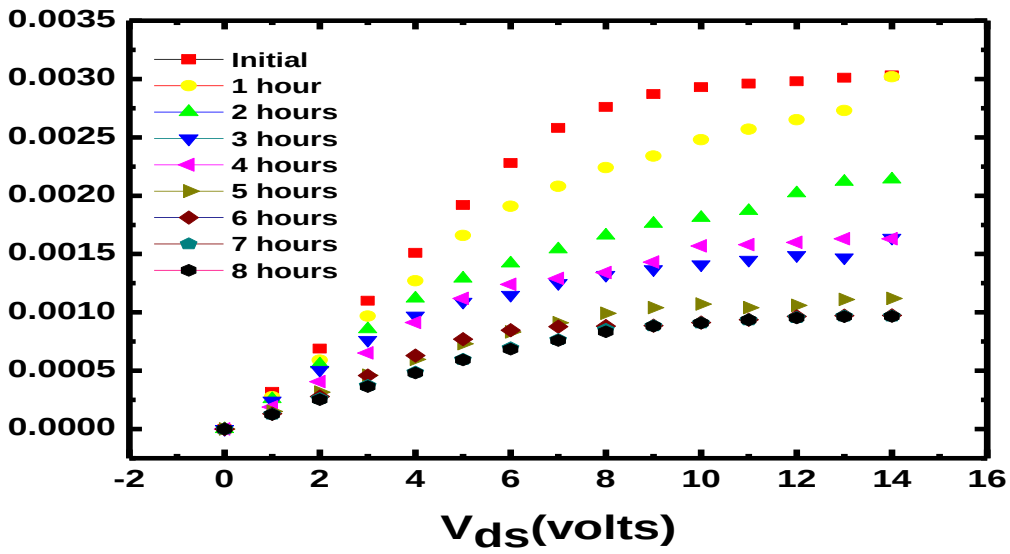

Figure 4.9: Decrease in drain current of the HEMT during the probe immobilization

The sensor surface is then rinsed with the immobilization buffer and is exposed to 1mM of mercaptohexanol for 90 minutes. The device is then exposed to 60µl of the hybridization buffer containing 4µM of the target DNA. The I_d-V_{ds} characteristics of the device are measured during this exposure. The Drain current of the HEMT decreases by as a function of time and stabilizes after 20 minutes. The decrease in drain current is 952 µA. This decrease is because the negative charge acting on the gate surface of the HEMT has increased due to the probe and the target binding between the probe and the target DNA[12] (Figure 10).

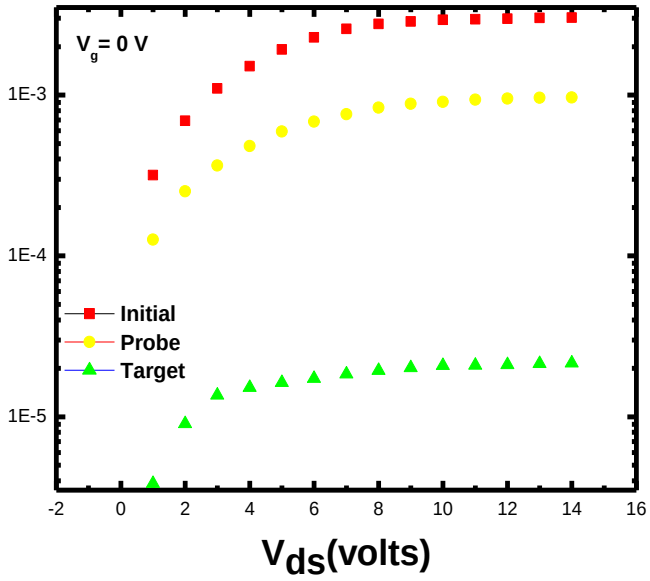

Figure 4.10: Decrease in the drain current of the HEMT during the probe immobilization and the target hybridization

The experiment was repeated with a probe and a target DNA concentration of 1µM keeping the other factors a constant. There was decrease in the drain current by 1010 µA during the probe immobilization and by 410µA during the probe- target hybridization. The decrease in the drain current was less than the decrease with the 4µM probe and target DNA. This trend is expected since a higher concentration of DNA results in a higher surface coverage density and thereby applying a larger negative potential on the gate contact.

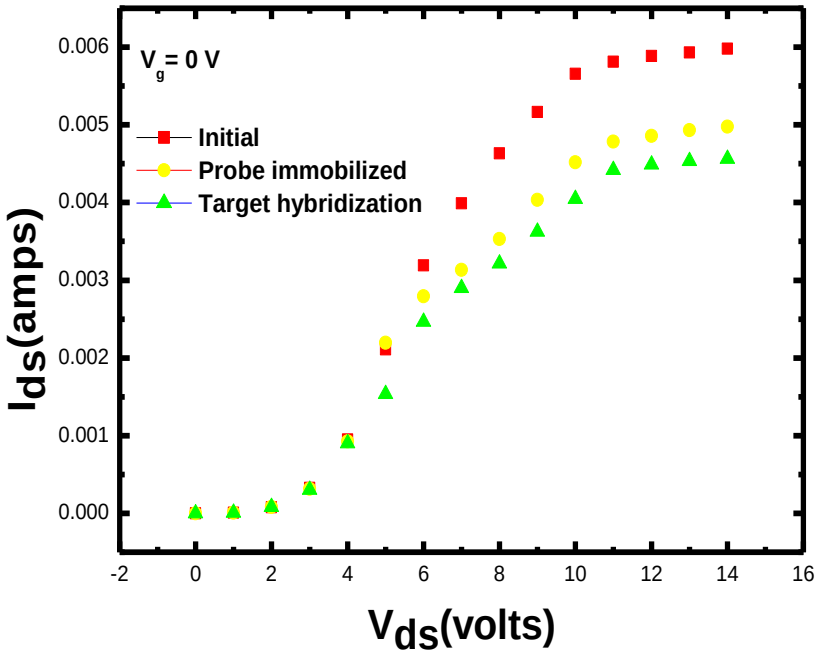

Figure 4.11: Decrease in drain current of the HEMT during probe immobilization and target hybridization with a 1µM concentration DNA

4.5 Conclusion

The key conclusions from this study are that it is possible to immobilize thiolated DNA on the gold surface of an AlGaN/GaN HEMT for the purpose of detection of DNA. Subsequently the immobilization can be monitored real time by measuring the I_{ds}- V_{ds} characteristics of the HEMT. More importantly this biosensor can also be used for continuous remote monitoring and analysis. There is a decrease in the drain current of the HEMT during the probe immobilization and probe and target hybridization.

The decrease in the drain current is larger with the higher concentration of thiolated DNA.

4.6 References

[1]V. Chan, S. E. McKenzie, S. Surrey, P. Fortina, D. J. Graves, J. Colloid InterfaceSci. **203,** 197 (1998). "Effect of hydrophobicity and electrostatics on adsorption of DNA oligonucleotides at liquid/solid interfaces"

[2]Y. Belosludtsev, B. Iverson, S. Lemeshko, R. Eggers, R. Wiese, S. Lee, T.Powdrill, M. Hogan, Anal. Biochem. **292** ,250 (2001). "DNA microarrays based on noncovalent oligonucleotide attachment and hybridization in two dimensions"

[3] C. Wittmann, Immobilisation o DNA on chips I. Germany, Springer, 2005.

[4] K. M. Rusin, T. L. Fare, J. Z. Stempe, Biosens. Bioelectron. **19**, 1537 (2004). "Immobilization of flavoproteins on silicon: effect of cross-linker chain length on enzyme activity"

[5]B. S. Kang, S. Kim, F. Ren, J. W. Johnson, R. Therrien, P. Rajagopal, J. Roberts, E. Piner, K. J. Linthicum, S. N. G. Chu, K. Baik, B. P. Gila, C. R. Abernathy, and S. J. Pearton, Appl. Phys. Lett. **87**, 172105 (2005). "Electrical detection of deoxyribonucleic acid hybridization with AlGaN / GaN high electron mobility transistors"

[6] Y. Ishige, M. Shimoda and M. Kamahori, Japan. J. Appl. Phys. **45**, 3776 (2006). "Immobilization of DNA probes onto gold surface and its application to fully electric detection of DNA hybridization using field-effect transistor sensor"

[7]I. Willner, E. Katz, Bioelectronics an Introduction. Wiley-VCH, 2005.

[8] S. L. McArthur, Surf. Interface Anal. 38 ,1380 (2006). "Applications of XPS in bioengineering"

[9] D. Y. Petrovykh, H. Kimura-Suda, L. J. Whitman and M. J. Tarlov, J. Am. Chem. Soc. **125**, 5219 (2003). "Quantitative Analysis and Characterization of DNA Immobilized on Gold"

[10] D. Y. Petrovykh, H. Kimura-Suda, L. J. Whitman and M. J. Tarlov, Langmuir, **20**, 429 (2004). "Quantitative Characterization of DNA Films by X-ray Photoelectron Spectroscopy"

[11]C. Y. Lee, H. E. Canavan, L. J. Gamble and D. G. Castner, Langmuir, **21**, 5134 (2005). "Evidence of Impurities in Thiolated Single-Stranded DNA Oligomers and Their Effect on DNA Self-Assembly on Gold"

[12] T. Sakata, M. Kamahori and Y. Miyahara, Jpn. J. Appl. Phys, **44**, 2854 (2005). "DNA Analysis Chip Based on Field-Effect Transitors"